

Fall 2012

Computational Modeling of Protein Dynamics with GROMACS and Java

Miaoer Yu
San Jose State University

Follow this and additional works at: https://scholarworks.sjsu.edu/etd_projects

Part of the [Computer Sciences Commons](#)

Recommended Citation

Yu, Miaoer, "Computational Modeling of Protein Dynamics with GROMACS and Java" (2012). *Master's Projects*. 267.

DOI: <https://doi.org/10.31979/etd.jkpw-3veg>

https://scholarworks.sjsu.edu/etd_projects/267

This Master's Project is brought to you for free and open access by the Master's Theses and Graduate Research at SJSU ScholarWorks. It has been accepted for inclusion in Master's Projects by an authorized administrator of SJSU ScholarWorks. For more information, please contact scholarworks@sjsu.edu.

**Computational Modeling of Protein Dynamics with
GROMACS and Java**

A Project

Presented to

The Faculty of the Department of Computer Science

San Jose State University

In Partial Fulfillment
of the Requirements for the Degree
Master of Computer Science

By

Miaoer Yu

December 2012

©2012

Miaoer Yu

ALL RIGHTS RESERVED

APPROVED FOR THE DEPARTMENT OF COMPUTER SCIENCE

Dr. Sami Khuri, Department of Computer Science, SJSU Date

Dr. Chris Pollett, Department of Computer Science, SJSU Date

Natalia Khuri, Bioengineering and Therapeutic Sciences, UCSF Date

ABSTRACT

Computational Modeling of Protein Dynamics with GROMACS and Java By Miaoer Yu

GROMACS is a widely used package in molecular dynamics simulations of biological molecules such as proteins, and nucleic acids, etc. However, it requires many steps to run such simulations from the terminal window. This could be a challenge for those with minimum amount of computer skills. Although GROMACS provides some tools to perform the standard analysis such as density calculation, atomic fluctuation calculation, it does not have tools to give us information on the specific areas such as rigidity that could predict the property of the molecules. In this project, I have developed a user friendly program to carry out molecular dynamics simulations for proteins using GROMACS with an easy user input method. My program also allows one to analyze the rigidity of the proteins to get its property.

ACKNOWLEDGMENTS

I would like to thank my project advisor Dr. Sami Khuri for countless suggestions and encouragement. I would also like to thank Dr. Chris Pollett for his suggestions and comments on my project. I am especially thankful to Natalia Khuri at UCSF, whose advice and ideas were essential to the completion of my project.

Table of Contents

| | |
|--|----|
| 1. Introduction to Molecular Dynamics Simulation | 7 |
| 2. GROMACS Overview | 13 |
| 3. Java Application Design and Implementation | 21 |
| 4. Applications | 32 |
| 5. Conclusions | 50 |
| 6. Future work | 51 |
| 7. References | 52 |

1. Introduction to Molecular Dynamics Simulation

Molecular dynamic simulation is a computational method that simulates the motion of a system of particles. McCammon introduced the first protein simulations in 1977, and since then this method has been widely used in the theoretical study of biological molecules including proteins and nucleic acids because it can provide molecular change information by calculating the time dependent behavior of a molecular system [1, 2]. For example, GROMACS is a package that carries out molecular dynamic simulations, and generates a trajectory of the molecule. GROMACS's high performance draws a lot of interest from researchers looking to develop their own tools to analyze the GROMACS trajectories. JGromacs, one of many applications written in the different languages from that used by GROMACS, analyzes the trajectories generated by GROMACS. JGromacs does not work with large molecules due to its huge memory consumption. In our project, we attempt to simplify the GROMACS steps, and develop our own analysis tool that works well with large molecules.

The goal of a molecular dynamics simulation is to predict macroscopic properties such as pressure, energy, heat capacities, etc. from the microscopic properties including atomic positions and velocities generated by molecular dynamic simulations. The bridge between macroscopic properties and microscopic properties is statistical mechanics using the time independent statistical average [1]. A molecular dynamics simulation generates a sequence of points in a multidimensional space as a function of time, where the points belong to the same collection of all possible systems which have different mechanical states such as positions or coordinates, and have the same thermodynamic state such as temperature, volume, pressure [1].

In statistical mechanics, an ensemble averages corresponding to experimental observables, and this means the molecular dynamics simulations must calculate all possible states of the system to get the ensemble averages [1]. "The Ergodic hypothesis, which states that the time average equals the ensemble average," allows the molecular dynamics simulation with enough representative conformations to calculate information on macroscopic properties using a feasible amount of computer resources [1].

In terms of classical mechanics, the molecular dynamics simulation is based on Newton's equation of motion:

$$\mathbf{F}_i = \mathbf{m}_i \mathbf{a}_i \quad (1.1)$$

where \mathbf{F}_i is the force acts on the particle, \mathbf{m}_i is the particle mass and \mathbf{a}_i is its acceleration. The force is also equal to the gradient of the potential energy:

$$\mathbf{F}_i = -\mathbf{dV} / \mathbf{dr}_i \quad (1.2)$$

where V is the potential energy of the system. The acceleration can be expressed as:

$$\mathbf{a}_i = \mathbf{d}^2 \mathbf{r}_i / \mathbf{dt}^2 \quad (1.3)$$

From equation 1.1, 1.2 and 1.3, we can relate the derivative of the potential energy to the changes in position as a time function:

$$-\mathbf{dV} / \mathbf{dr}_i = \mathbf{m}_i \mathbf{a}_i = \mathbf{m}_i (\mathbf{d}^2 \mathbf{r}_i / \mathbf{dt}^2) \quad (1.4)$$

When the acceleration, \mathbf{a} , is constant:

$$\mathbf{a} = \mathbf{dv} / \mathbf{dt} \quad (1.5)$$

$$\mathbf{v} = \mathbf{at} + \mathbf{v}_0 \quad (1.6)$$

$$\mathbf{v} = \mathbf{dx} / \mathbf{dt} \quad (1.7)$$

From the combination of 1.5, 1.6 and 1.7, we obtain the relation of \mathbf{x} and the acceleration, \mathbf{a} , the initial position, \mathbf{x}_0 , and initial velocity, \mathbf{v}_0 at time t :

$$\mathbf{x} = \mathbf{at}^2 + \mathbf{v}_0 \mathbf{t} + \mathbf{x}_0 \quad (1.8)$$

From equation 1.4, the acceleration is the derivative of the potential energy with respect to the position, \mathbf{r} :

$$\mathbf{a} = (-dE/dr) / m \quad (1.9)$$

We can obtain the initial positions of the atoms from experimental structures, such as the x-ray crystal structure of the molecule, the acceleration from the gradient of the potential energy function, and the initial distribution of velocities from:

$$\mathbf{P} = \sum_{i=1}^N \mathbf{m}_i \mathbf{v}_i = \mathbf{0} \quad (1.10)$$

where \mathbf{P} is momentum, \mathbf{v}_i is the velocities that are often chosen randomly from a Maxwell-Boltzmann or Gaussian distribution at a given temperature [1].

The potential energy is a function of the atomic positions of all the atoms in the system. Because this function is complicated, it must be solved numerically with numerical algorithms such as Verlet algorithm, Leap-frog algorithm, Velocity Verlet, Beeman's algorithm, etc [1].

In [1], those algorithms are introduced. "All of those algorithms assume the positions, velocities and accelerations can be approximated by a Taylor series expansion:

$$\mathbf{r}(t + \delta t) = \mathbf{r}(t) + \mathbf{v}(t)\delta t + (1/2)\mathbf{a}(t) \delta t^2 + \dots \quad (1.11)$$

$$\mathbf{v}(t + \delta t) = \mathbf{v}(t) + \mathbf{a}(t)\delta t + (1/2)\mathbf{b}(t) \delta t^2 + \dots \quad (1.12)$$

$$\mathbf{a}(t + \delta t) = \mathbf{a}(t) + \mathbf{b}(t)\delta t + \dots \quad (1.13)$$

where \mathbf{r} is the position, \mathbf{v} is the velocity, \mathbf{a} is the acceleration, etc."

For example, to derive the Verlet algorithm, we can write:

$$\mathbf{r}(t + \delta t) = \mathbf{r}(t) + \mathbf{v}(t)\delta t + (1/2)\mathbf{a}(t)\delta t^2 \quad (1.14)$$

$$\mathbf{r}(t - \delta t) = \mathbf{r}(t) - \mathbf{v}(t)\delta t + (1/2)\mathbf{a}(t)\delta t^2 \quad (1.15)$$

Combining 1.14 and 1.15, we obtain:

$$\mathbf{r}(t + \delta t) = 2\mathbf{r}(t) - \mathbf{r}(t - \delta t) + \mathbf{a}(t)\delta t^2 \quad (1.16)$$

This algorithm uses positions and acceleration at time t and the positions from time $t - \delta t$ to calculate the new positions at time $t + \delta t$.

The available potential energy functions such as the AMBER, CHARMM, GROMOS, OPLS / AMBER, etc. provide reasonably good accuracy with reasonably good computational efficiency [1]. Therefore, we have the needed information to calculate the trajectory that describes the positions, velocities and acceleration of the particles at different time, and we can determine the detailed information about the molecules [1].

In general, there are three stages in molecular dynamics simulation: preparation of the input, production molecular dynamics, and analysis of the result (Figure 1) [3].

Stage I: Preparation

This stage has multiple steps including generating the topology file; defining a box and filling it with solvent, and adding any counter-ions to neutralize the system; performing energy minimization to provide stable simulation; performing equilibration for sufficient time to get stable pressure, temperature and energy [3].

Stage II: Production

This stage is the longest stage resulting in a trajectory containing coordinates and velocities of the system.

Stage III: Analysis

The last stage includes analysis of the resulting trajectory and data files to obtain information on the property of the molecule. Some important quantities calculated in this stage include RMS difference between two structures, RMS fluctuations, and rigidity or constant force, etc. The equations used to calculate those quantities are listed as the following [1, 4]:

RMS difference between two structures

$$\mathbf{RMSD} = \langle (\mathbf{r}_i^\alpha - \mathbf{r}_i^\beta)^2 \rangle^{1/2} = \left((1/N_i) \sum_i (\mathbf{r}_i^\alpha - \mathbf{r}_i^\beta)^2 \right)^{1/2} \quad (1.17)$$

RMS fluctuations

$$\mathbf{RMSF} = \left((1/N_f) \sum_F (\mathbf{r}_i^f - \mathbf{r}_i^{\text{avg}})^2 \right)^{1/2} \quad (1.18)$$

Rigidity or force constant, k_i , where i represents amino acid in a protein:

$$\mathbf{k}_i = 3\mathbf{K}_B\mathbf{T} / \langle (\mathbf{d}_i - \langle \mathbf{d}_i \rangle)^2 \rangle \quad (1.19)$$

where \mathbf{K}_B is Boltzmann coefficient, \mathbf{T} is temperature in the simulation, \mathbf{d}_i is the average distance of $\mathbf{C}_{\alpha i}$ from other $\mathbf{C}_{\alpha i}$ in the protein excluding \mathbf{C}_{α} s of the immediate neighbors, and $\langle \mathbf{d}_i \rangle$ is the same as \mathbf{d}_i but averaged over the entire simulation [4].

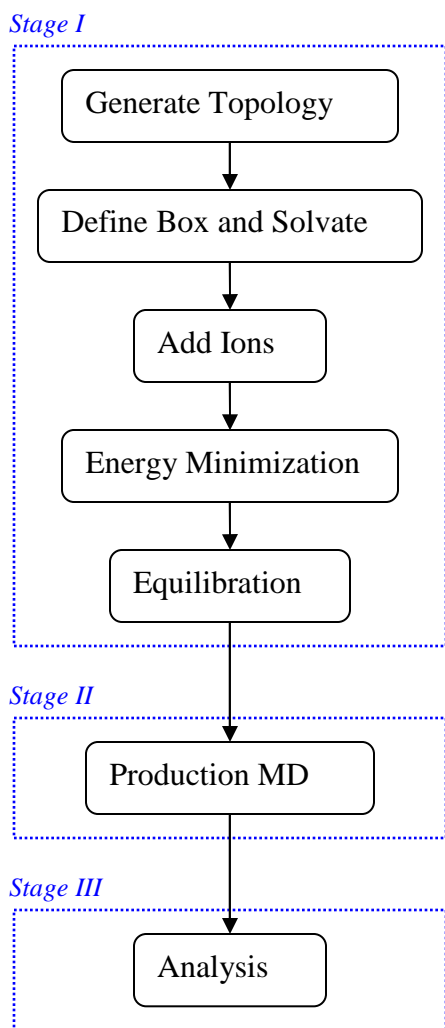


Figure 1. Three stages in molecular dynamic simulation: preparation of the input, production molecular dynamic and analysis of the result.

Among many molecular dynamics simulation packages, GROMACS, CHARMM, AMBER, and NAMD are most commonly used [5]. We will use GROMACS in our study because it is open-source, and popular in the study of protein. Before we develop a tool to analyze the GROMACS data, we need to understand GROMACS. In the next section, we will introduce GROMACS and its features.

2. GROMACS Overview

GROMACS is an acronym for GRONingen Machine for Chemical Simulation. It was developed at the University of Groningen, The Netherlands, in the early 1990s [6]. This open-source project is written in ANSI C, and contains about 100 utility and analysis programs which allow users to perform molecular simulations and energy minimization (EM) for biological molecules [6]. It is one of the most commonly used molecular dynamics simulation packages. The following is a list of the main features the GROMACS has [7, 8].

1. Features for generating topologies and coordinates [7, 8]
 - pdb2gmx – converts pdb files to topology and coordinate files.
 - editconf – edits the box and writes subgroups
 - genbox – solvates a system
 - genion – generates mono atomic ions on energetically favorable positions

2. Features for running a simulation [7, 8]
 - grompp – makes a run input file
 - mdrun – performs a simulation, does a normal mode analysis or an EM.

3. Features for processing properties [7, 8]
 - g_energy – writes energies to xvg files and displays averages
 - g_gyrate – calculates the radius of gyration
 - g_potential – calculates the electrostatic potential across the box
 - g_density – calculates the density of the system

4. Features for processing files [7, 8]
 - trjconv – converts and manipulates trajectory files

5. Analysis tools [7, 8]
 - g_rms – calculates rmsd's with a reference structure and rmsd matrices

`g_rmsf` – calculates atomic fluctuations

The typical GROMACS MD run of the protein such as lysozyme is demonstrated in the flow chart (Figure 2) [7, 8]. In the flow chart, the steps are listed in the left column, while the highlighted GROMACS tools are listed in the right column corresponded to the left column.

To learn how to use GROMACS in MD of the protein, we followed the tutorial for lysozyme [9]. In this example, PDB file 1AKI.pdb can be downloaded from RCSB website for hen egg white lysozyme (PDB code 1AKI). The `pdb2gmx` generates a topology for the molecule, the position restraint file, and a post-processed structure file.

The lysozyme is simulated in a simple aqueous system. The `editconf` tool defines the box dimensions, and the `genbox` tool fills the box with water. The purpose of the `genbox` is to keep track of the number of added water molecules, and update the topology with the changes [7, 8]. Now the system is solvated and contains a charged protein.

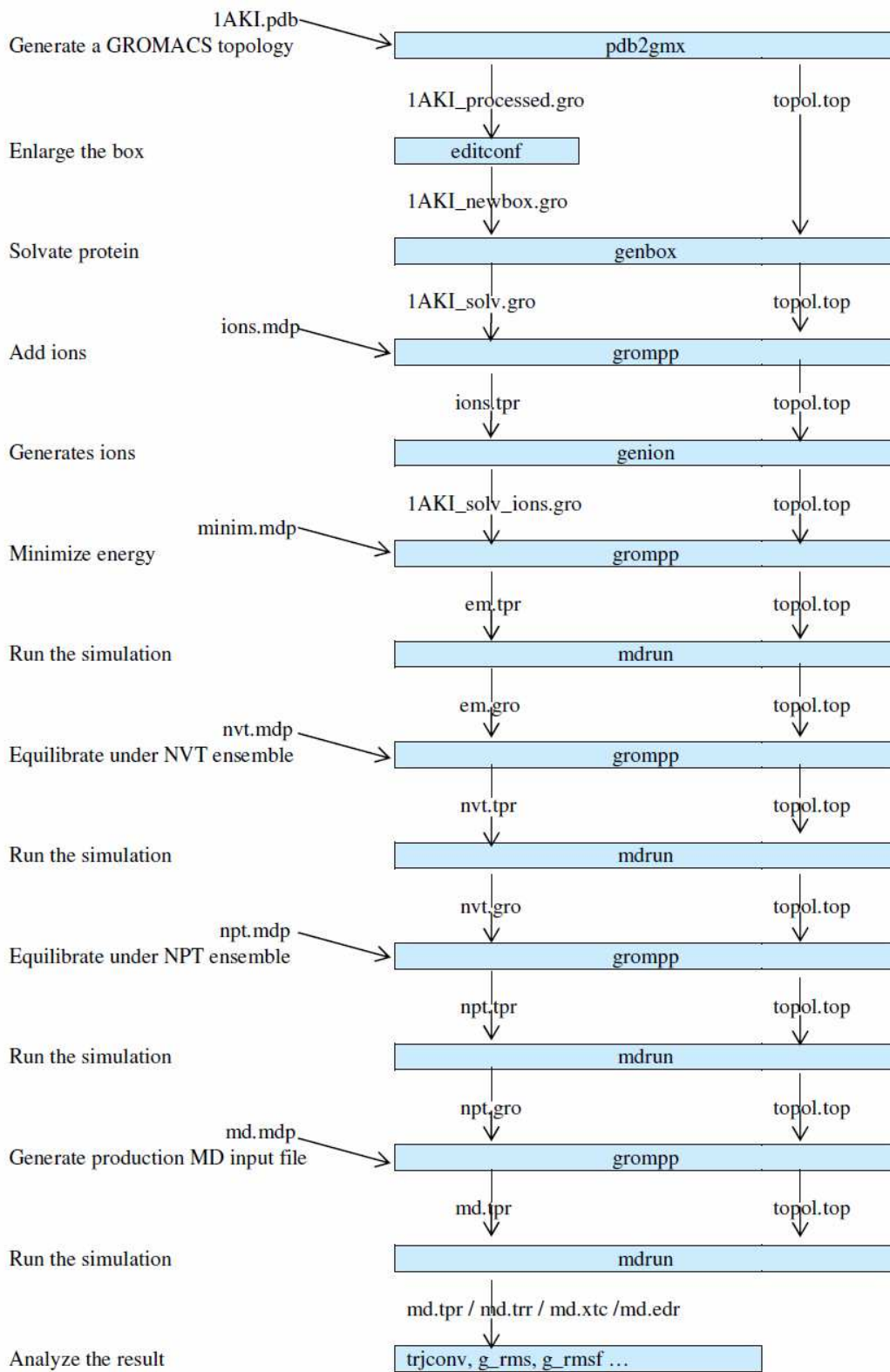


Figure 2. Flow chart of lysozyme GROMACS MD run. Adapted from GROMACS Reference [7].

The tool grompp (GROMACS pre-processor) processes the ions.mdp (molecular dynamics parameter file), the coordinate file and topology to generate an atomic-level input (ions.tpr) containing all the parameters for all of the atoms in the system. The genion tool reads through the topology and replaces water molecules with the ions specified by the user to neutralize the net charges on the protein [9].

The energy minimization relaxes the structure to ensure that the system has no steric clashes or inappropriate geometry [9]. The tool grompp assembles the minim.mdp, the structure, topology to generate an input file (em.tpr), and then the tool mdrun runs the energy minimization to generate an energy-minimized structure file em.gro, energy file em.edr and trajectory em.trr. The analysis of em.edr file with the tool g_energy results in the following graph showing the steady convergence of $E_{\text{potential}}$ (Figure 3) [9].

Energy Minimization for Lysozyme (1AKI)

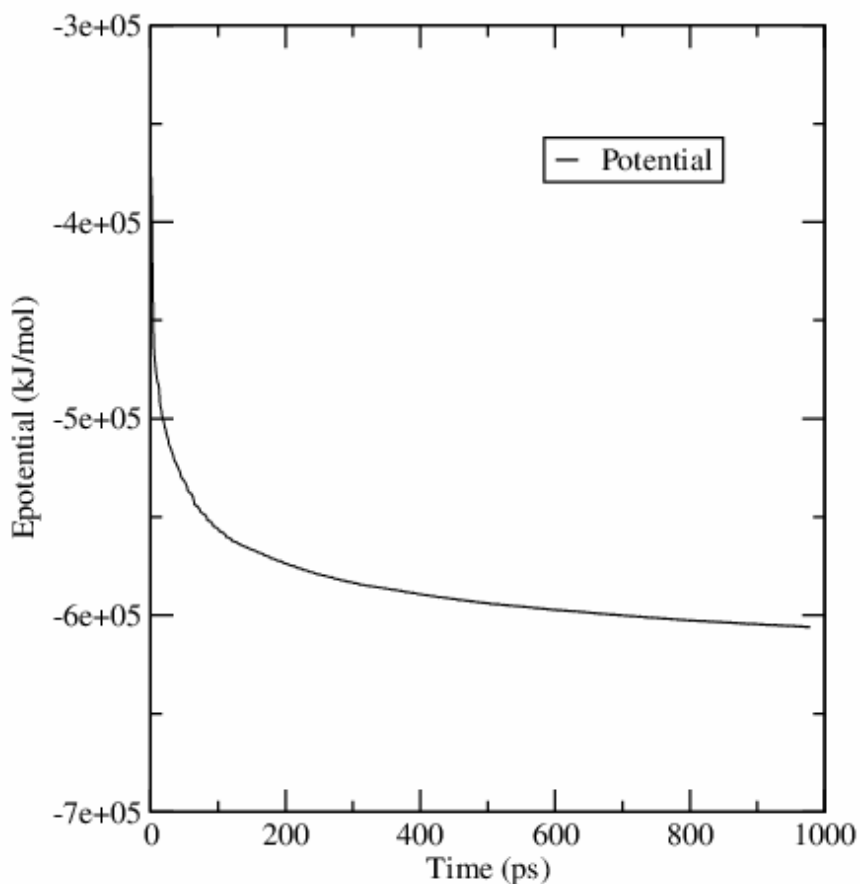


Figure 3. Energy Minimization for Lysozyme (1AKI).

Once we get the reasonable starting structure, we need to equilibrate the solvent and ions around the protein under an NVT ensemble (the constant Number of particles, Volume, and Temperature) and an NPT ensemble (the constant Number of particles, Pressure, and Temperature) [9]. The same tools used in EM step perform the two-phase equilibration. The tool `g_energy` processes the result to generate plots for NVT (Figure 4) and NPT (Figure 5) [9].

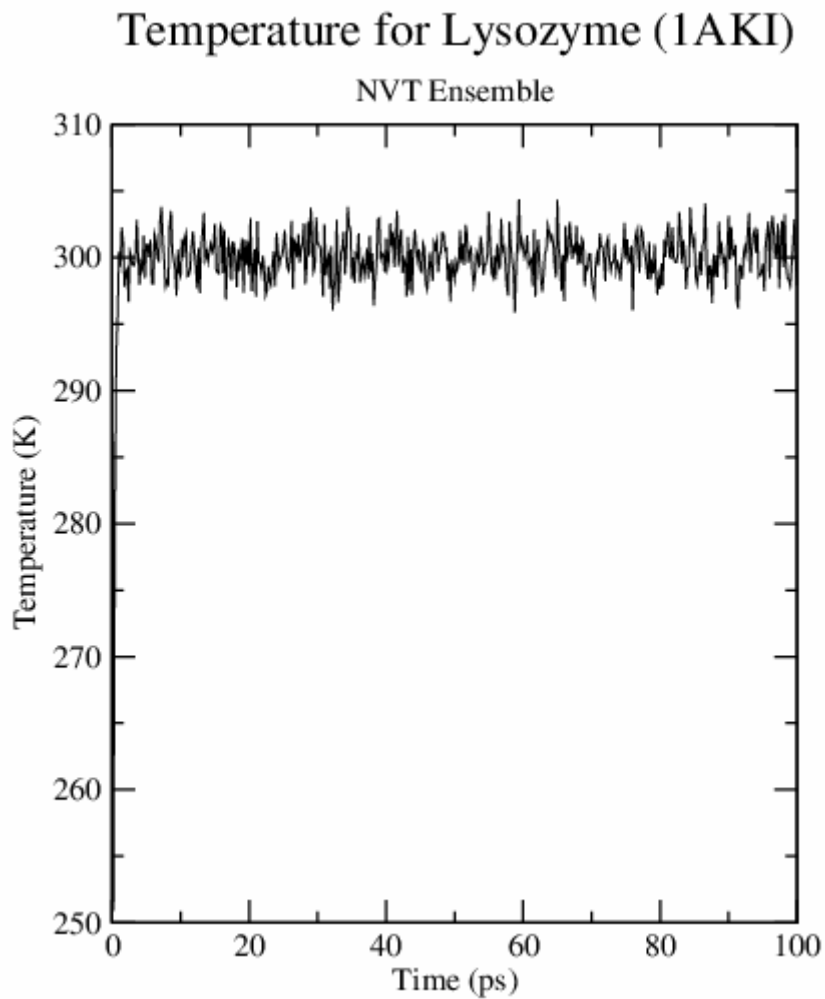


Figure 4. Temperature for Lysozyme (1AKI).

Figure 4 shows that the system reaches the target temperature, and stays there over the remainder of the equilibration. Figure 5 has the fluctuated pressure value. However, the running average of these data is stable [9].

After finishing the preparation stage, the previous tools grompp and mdrun are used to perform the production MD to generate the final trajectory file md.trr and md.xtc etc.

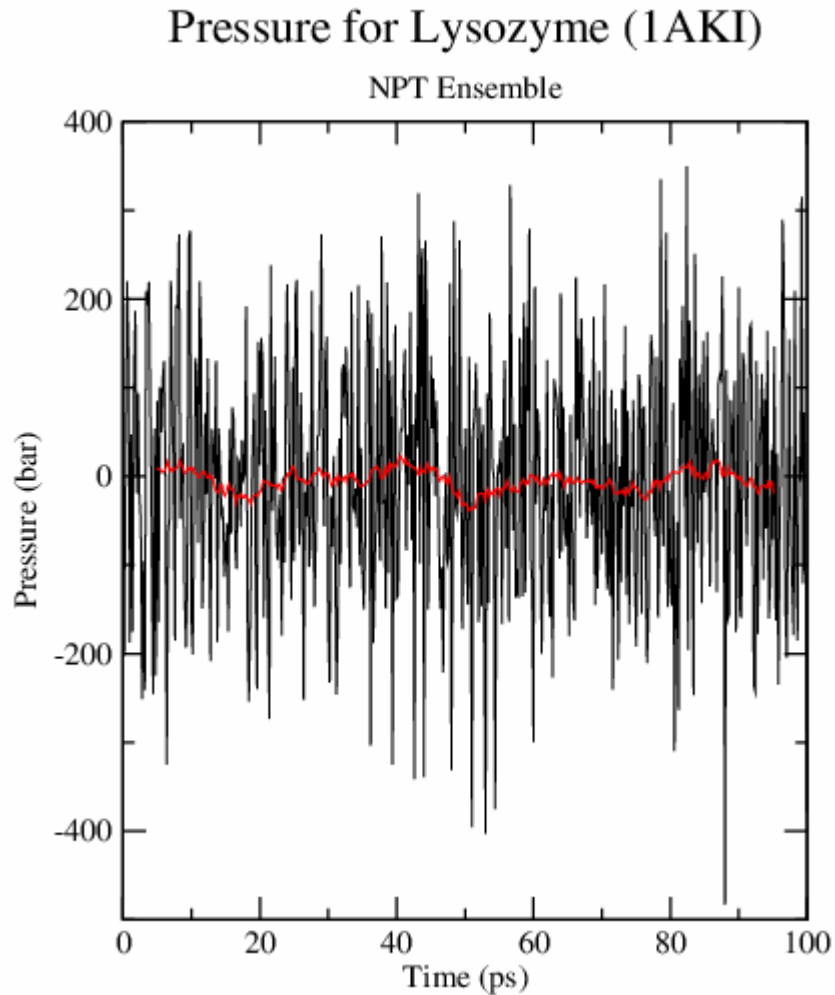


Figure 5. Pressure for Lysozyme (1AKI).

After finishing the simulation, we can analyze the system with GROMACS tools trjconv, g_rms, g_rmsf, etc. The RMSD plot obtained with the tool g_rms (Figure 6) shows that the structure is very stable with stable RMSD. The RMSF plot obtained with the tool g_rmsf (Figure 7) shows how each residue fluctuates during the period of the production run [9].

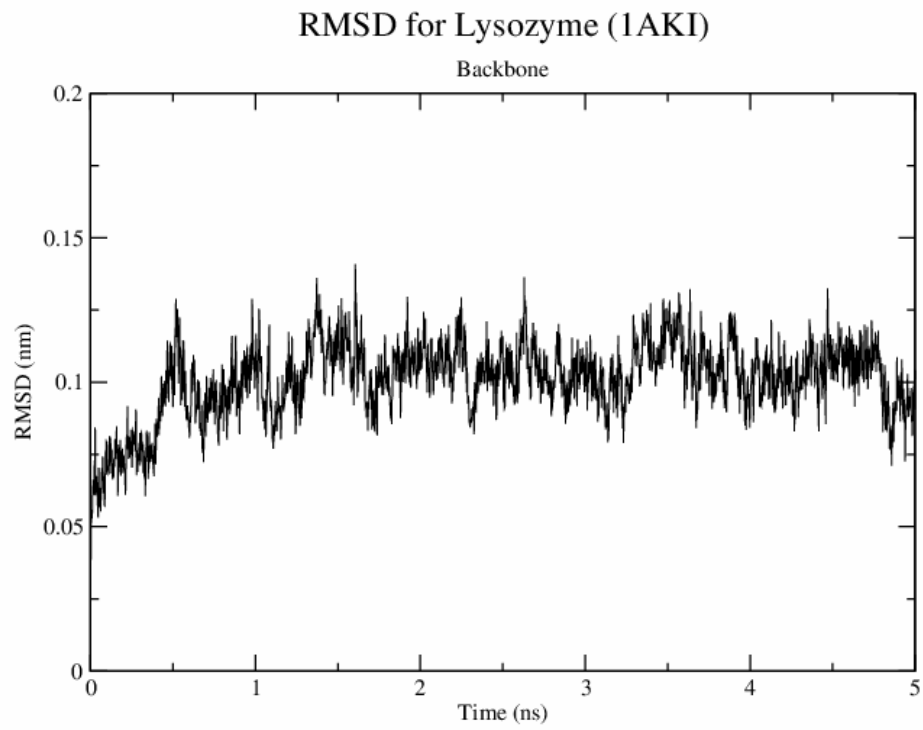


Figure 6. RMSD for Lysozyme (1AKI)

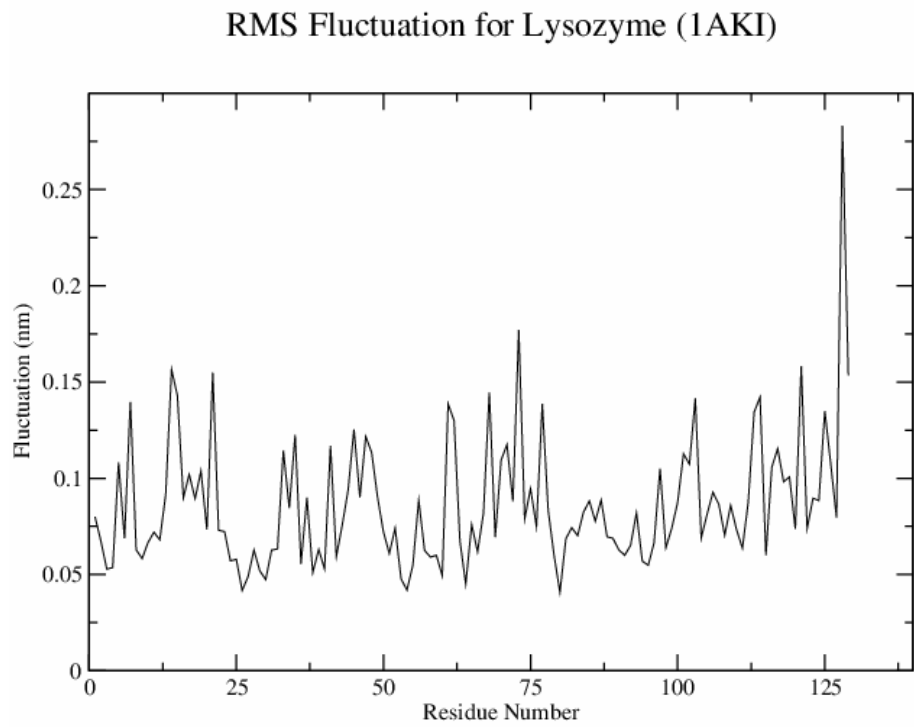


Figure 7. RMS Fluctuation for Lysozyme (1AKI).

As shown in Figure 2, there are many steps involved in the whole process of molecular dynamics simulation. Some users may find it difficult to use the GROMACS from a terminal window. On the other hand, GROMACS provides some tools to perform the basic analysis of the trajectories, but we could not find tools to give us the information on the specific areas such as rigidity we are interested in due to its relation to the protein property [4]. In the next section, we will show the development of a Java program that simplifies the GROMACS steps through GUIs and processes the trajectories to give rigidity information of the protein.

3. Java Program Design and Implementation

The two goals in this project are to simplify the MD running steps in GROMACS with GUIs, and to create an analysis tool that processes the GROMACS trajectories and gives us the rigidity profile of the proteins.

GROMACS is written in the C language, but we will develop our program in Java. Therefore, we investigated two methods that allow Java to use the codes and code libraries written in other languages such as C. One involves the Java Native Interface (JNI), and another involves Java Runtime class. The former requires six steps to call C from Java code [10]:

1. Create the Java code. The code needs to have declaration of the native method, load the shared library containing the native code, and then call the native method.
2. Compile the Java code
3. Create the C header file by running `javah -jni` command on the java code
4. Create the C code
5. Compile the C code and create shared library
6. Execute Java program.

The latter involves creating an object of Runtime, and this Runtime object calls the Runtime method `exec(command)` where the command can be used to call C functions. Some codes related to the script call in Runtime are as follows:

```
Runtime rt = Runtime.getRuntime(); //create an object rt of Runtime
String[] cmds = {scriptName, parm1, parm2}; //command to execute the script
Process process = rt.exec(cmds); //create a process object
process.waitFor(); //wait for the script completion
```

Since the former is more complicated to implement, we use the latter in our program.

We built the GUIs with the Model-View-Controller (MVC) pattern first described by Krasner and Pope for building user interfaces in Smalltalk-80 [11]. In MVC, the model contains data and some tasks, the view presents the data to the user, and the controller updates the model as necessary when the user interacts with the view [12]. The separation

of the three components makes it easy to reuse and maintain the codes. In our program, we combine the view and the controller in the same class, but separate the data from the presentation. Due to its large library, containing lots of reusable codes, we wrote the program in Java, and have our Model to extend the java class Observable that provides the register/notify infrastructure needed to support the views implementing the java interface Observer [12]. When the view sees a user interaction, the listeners registered by the controller are called, and then the controller calls the mutator methods of the model to update its state, and the model calls `setChanged()` and `notifyObservers()` after it has changed the state. `NotifyObservers()` will notify the registered observer that the change has been made, and the observer containing the required update method will make the change to itself [12].

The class diagram of the project is illustrated in Figure 8. Our program consists of three subpackages including task, data and gui. The task package contains the classes for distance calculation, rigidity calculation and the regular file processing; the data package contains the classes that represent the binary structural data such as the trajectory file, structure file, etc. and the gui package contains the different view/controller classes that allow users to enter their settings for the simulations, and the model class that stores the user inputs.

The program communicates with the users for their inputs starting with `MainPanelView` class. The `MainPanel` view is illustrated in Figure 9.

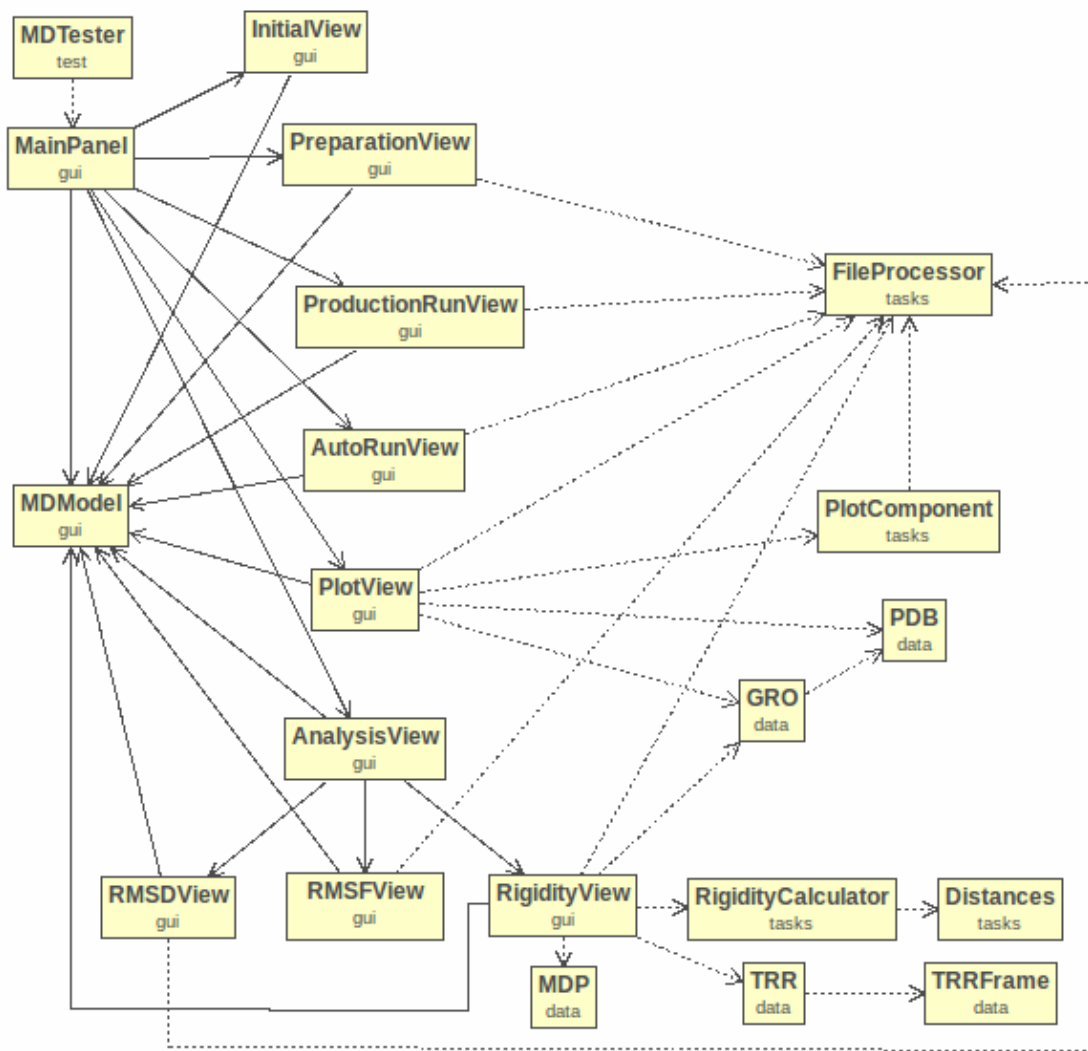


Figure 8. UML class diagram of the project.

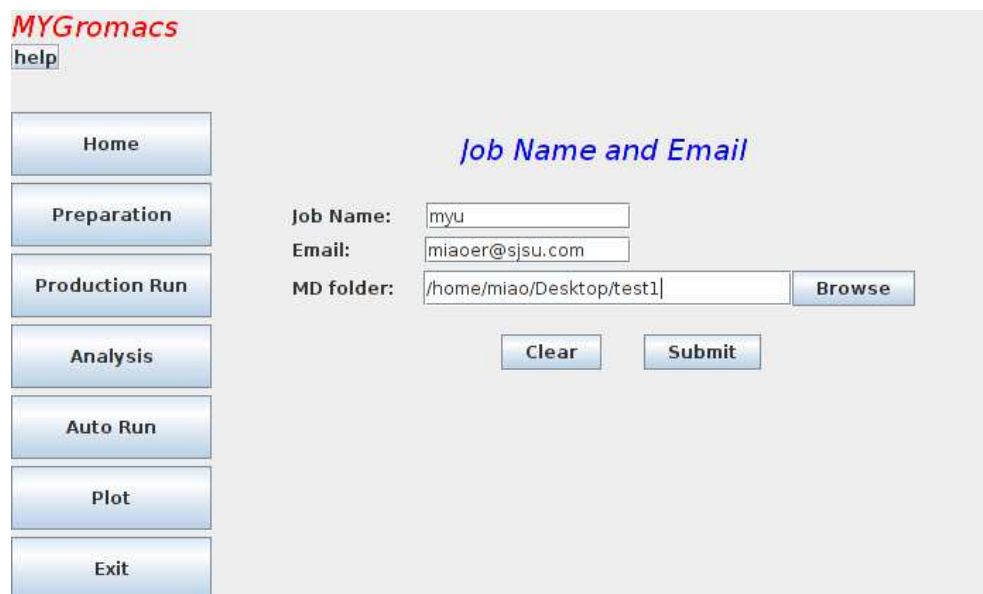


Figure 9. Initial panel view.

Six function buttons including “Home”, “Preparation”, “Production Run”, “Auto Run”, “Plot”, and “Exit” are listed on the left column of the page, and the help function button is in the upper left corner. The user can select the specific function by clicking on the button labeled with the name of the function. After the user selects the function, the corresponding page will be displayed for the user inputs.

When the user clicks on Home, Figure 9 is displayed. The user enters the MD folder, and the program later will store the files created during the MD preparation and production.

When the user clicks on Preparation, the Preparation page will be displayed for the required and optional files and parameters (Figure 10). The user can either provide the pdb file or the PDB code of the protein. If the user gives both, the pdb file will be used. Four mdp files including ions mdp, EM mdp, NVT mdp and NPT mdp are required in this stage. If the user does not specify the file paths, we will use the default files contained in the package.

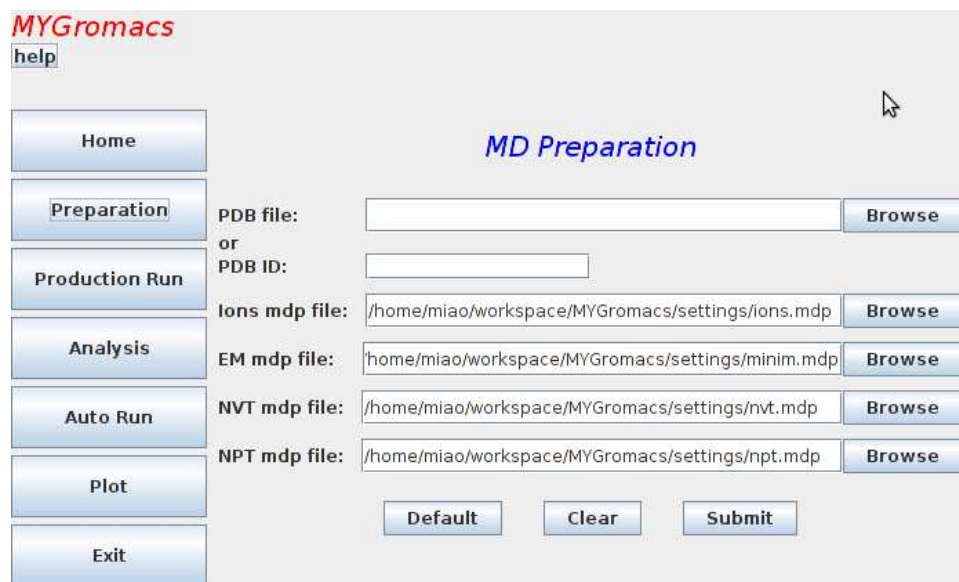


Figure 10. PreparationView panel.

When the user clicks on Production run, the MD Production page will be displayed for the required and optional files and parameters (Figure 11). If the user does not provide the file paths, we will use the default MD mdp contained in the package, and the NPT gro file, topology resulting from the preparation stage in the MD folder, and default options and output tpr file name.

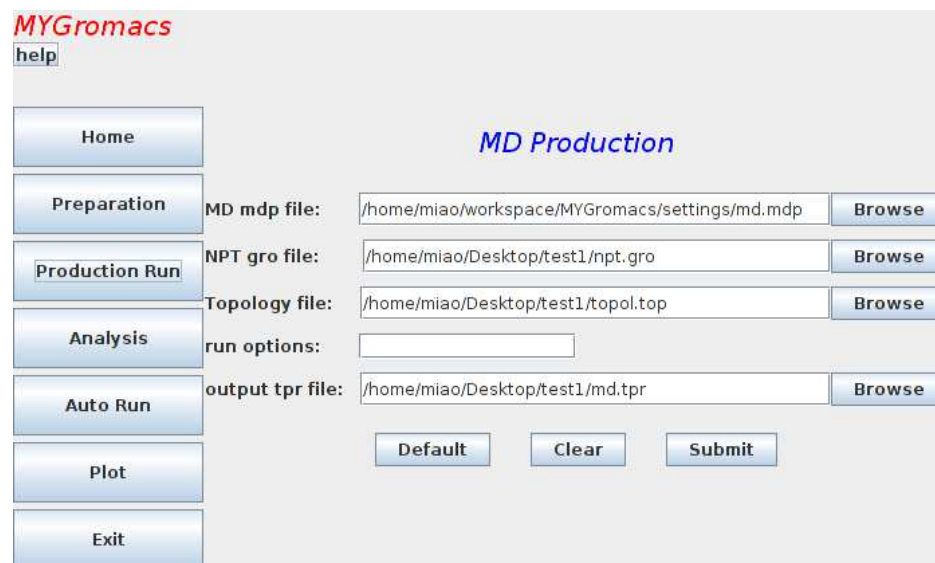


Figure 11. ProductionView panel.

When the user clicks on Analysis, the analysis page will display three basic analysis tools (Figure 12). If the user clicks on RMSD, RMSF, or Rigidity, the corresponding tool page will be displayed under the analysis page (Figure 13, Figure 14, and Figure 15).

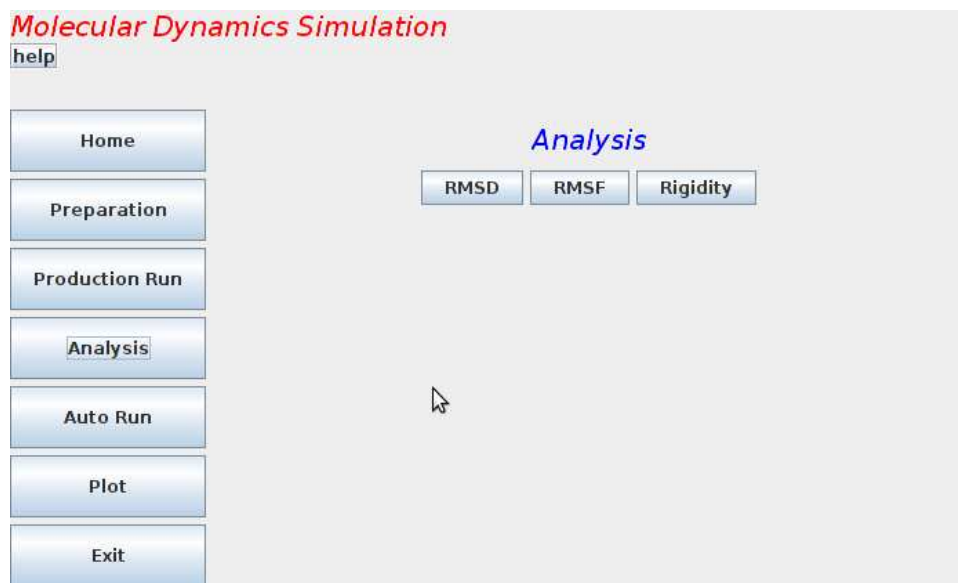


Figure 12. AnalysisView panel.

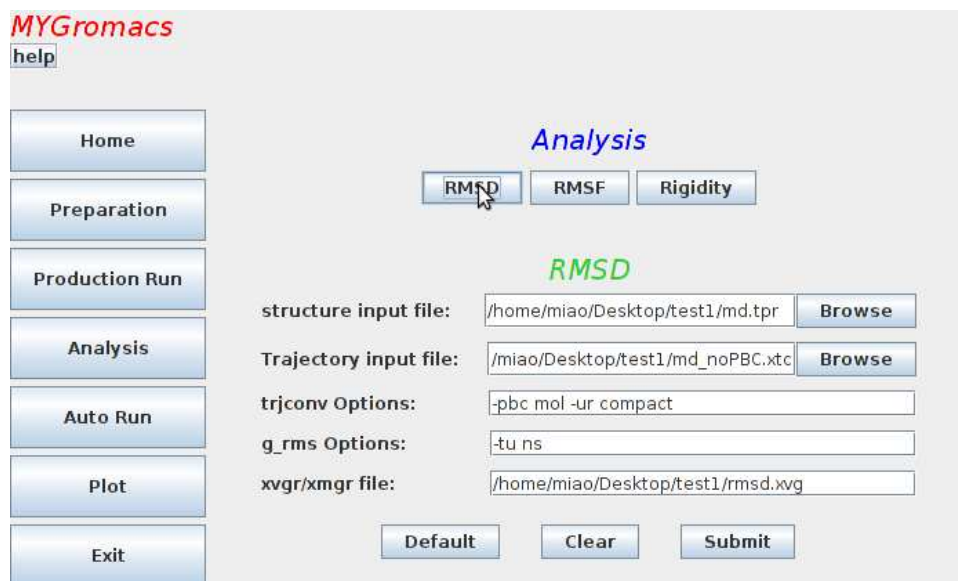


Figure 13. RMSDView panel.

The RMSD view also displays the default options, and the output xvg file name.

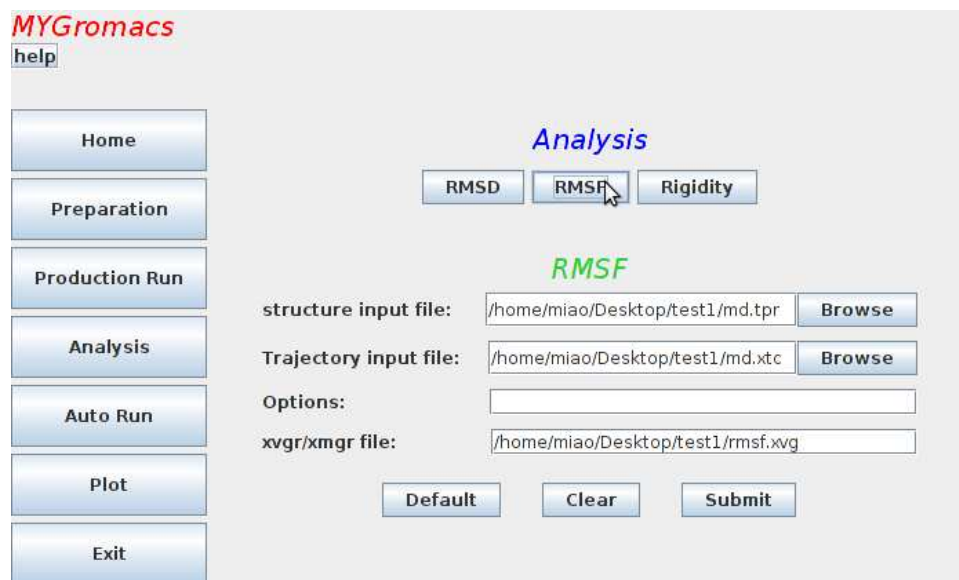


Figure 14. RMSFView panel with default output xvgr file name.

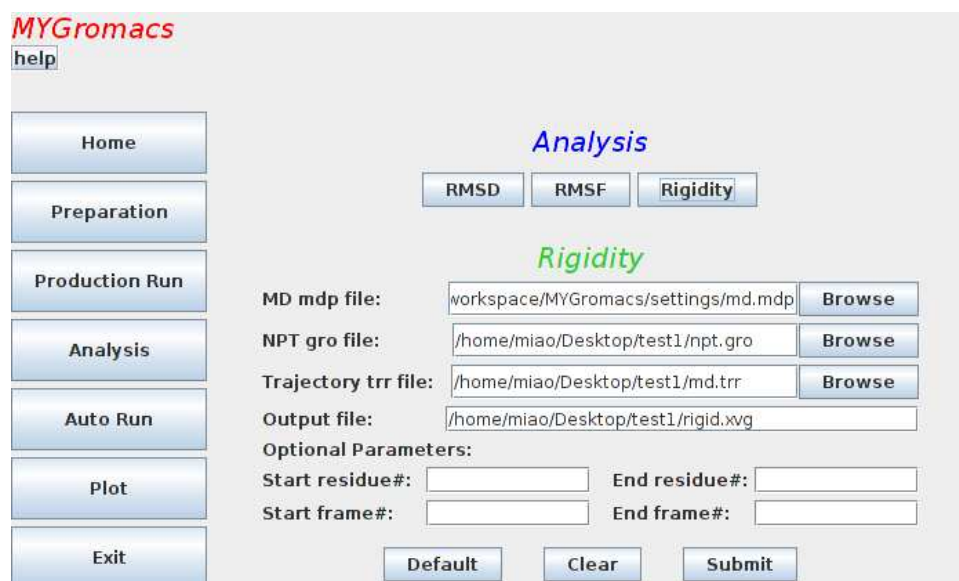


Figure 15. RigidityView Panel.

The rigidity view allows the users to choose the region of the protein they want to study, or/and the frames they want to consider since the frames at the beginning of the simulation are not stable and could be ignored. If the users don't provide any input, we

will use the default mdp file, the NPT gro file, and the trajectory file resulting from the previous MD run.

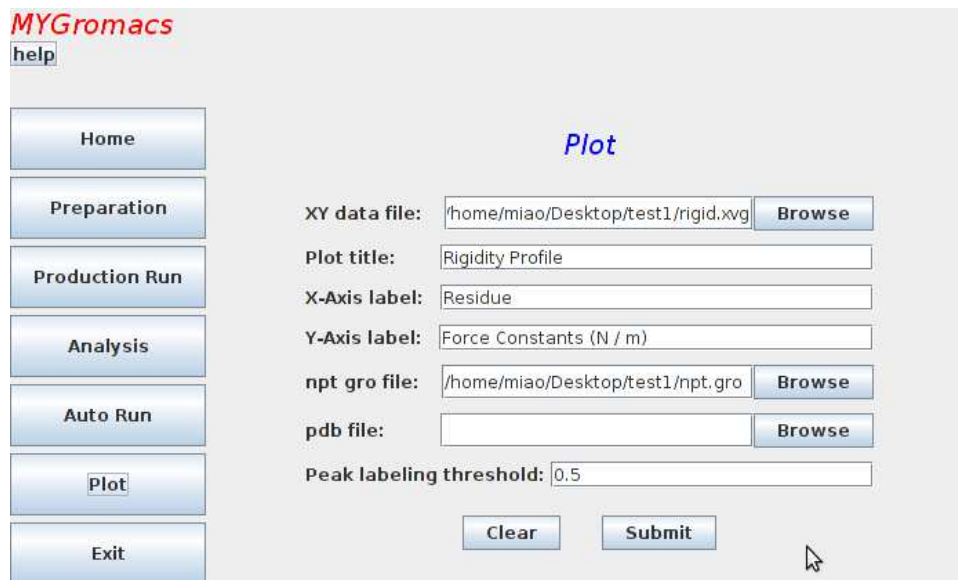


Figure 16. PlotView panel.

When the user clicks on the Plot button, the user is asked to input the data file, and the program displays the requested rigidity profile plot labeling the amino acids with high rigidity (Figure 16). If the user wants to take the default settings, he/she can click on the Auto Run button, and then enter the pdb file or pdb code on the corresponding page. The program will run the steps included in preparation and production stages with the default settings. The user can exit the program by clicking the exit button.

To simplify the MD process, we prepared scripts that execute the MD steps (see Attached CD). After the user enters the input or takes the default values, and then clicks on the submit button, the program will run the scripts in Java Runtime. It is crucial to realize that although GROMACS is written in the C language, Java Runtime class allows users to conduct their GROMACS research in a Java environment. In this way, the user does not need to exit the program to have a MD run in another environment.

The second goal of this project is to process the trajectories to get the rigidity profile of the protein. As mentioned before, we use Boltzmann coefficient and the distance of the

backbone carbon (C_α) of the protein from other backbone carbons (C_α s) in the protein in the calculation of the rigidity.

We need to obtain the coordinate information from the binary structural data file containing the trajectories, and then use the information to calculate the rigidity of the protein. The resulting rigidity profile can be used to describe the mechanical properties of the protein.

There are many packages, such as Biojava, StatAlign, Jmol and JGromacs, written in Java for bioinformatics analysis [5]. Among those packages, JGromacs has a much smaller API because it is designed to focus on the specific functionalities such as analyzing GROMACS trajectories [5]. We thought we would find the right tool for reading the GROMACS trajectory file to get the coordinate information of the alpha carbons. However, it has very low performance when it processes the large trajectory file of the large protein. We successfully used JGromacs to process the trajectory file of lysozyme that has 129 amino acids. However, when we ran the simulation with longer proteins that are more than 600 residues long, the computer took much longer, and the resulting trajectory file is much larger.

JGromacs parses the trajectory file via the use of GROMACS tool `gmxdump` with Java Runtime class. What the `gmxdump` does is to read a trajectory file and print that to standard output in a readable format [7]. JGromacs calls the `gmxdump` function and reads the information from the standard output, and then stores the information in memory. In general, MD simulations of proteins generate a huge trajectory file. When we incorporate JGromacs in our package, the machine is very slow with a small protein or hangs with a large protein. We cannot use JGROMACS in our program due to its low performance in input/output (IO) caused by huge memory consumption.

To get the coordinates of the alpha carbons of the protein, we must find an efficient way to read the trajectory file. The file with `trr` file extension contains the trajectory of a simulation. All the coordinates, velocities, forces and energies are printed as specified in the `mdp` file. The `trr` file in GROMACS contains many frames of data, and each frame has the same data structure as follows [7]:

```
int magic; // magic number
```

```

int sLen; // the String version length
int linefeed; // line feed
String version = ""; // version
int ir_size; // Backward compatibility
int e_size; // Backward compatibility
int box_size; // Non zero if a box is present
int vir_size; // Backward compatibility
int pres_size; // Backward compatibility
int top_size; // Backward compatibility
int sym_size; // Backward compatibility
int x_size; // Non zero if coordinates are present
int v_size; // Non zero if velocities are present
int f_size; // Non zero if forces are present
int natoms; // The total number of atoms
int step; // Current step number
int nre; // Backward compatibility
float t; // Current time
float lambda; // Current value of lambda
float [][] box;
float [][] vir;
float [][] pres;
float [][] coordinates;
float [][] velocities;
float [][] forces;

```

From the MD mdp file, we can calculate the total number of frames stored in the trajectory file with formula:

$$\text{Total number of frames} = \text{nsteps} / \text{nstxout} + 1$$

where nsteps and nstxout are the parameters found in the MD mdp file. With Java API, we can easily get the size of the trr file in bytes, and hence a frame in bytes. Therefore, we can know the offset of each frame in the file. The offset, the data structure of the frame, and the alpha carbon index obtained from the NPT gro file allow us to get the coordinate information of the alpha carbons.

To solve the memory consumption problem found in JGromacs, we load one frame of information to the buffer at a time, extract the coordinate data of the alpha carbons, and

then store the coordinates in an array. In this way, the size of the data we process is very small. Hence, the performance is increased.

To compare the performance between the JGROMACS and our method in getting the coordinate information, we wrote a small program to get the information from a trajectory file with JGROMACS's strategy since we can not directly use JGROMACS due to its exception with large protein. The following table demonstrates the performance of two methods on getting the coordinates of the alpha carbons from a trr file of size 13G resulting from the 10 ns molecule dynamics simulation of PCSK9 protein (Table 1).

Table 1: Comparison of two methods

| | JGROMACS Method | MYGromacs Method |
|---------------|-----------------|------------------|
| Time (second) | 5008 | 102 |

The result indicates our method increases the performance about 50 times.

In summary, we improve the performance by two strategies: to divide the large amount of structural data into frames of data and process one frame of data at a time; and to limit the number of objects created for each entry in the trajectory file by storing the information in an array. The codes are documented in the attached CD.

In the next section, we will demonstrate the rigidity profile of the lysozyme and compare its property with the RMS fluctuation property obtained from the GROMACS tool. After we confirm the reliability of our program with the well studied lysozyme, we will perform the similar study on the PCSK9 compounds that play important roles in cholesterol metabolism.

4. Applications

I. PCSK9 Introduction

Cholesterol is an important component of cellular membranes and is a precursor of steroid hormones and bile acids. It has been extensively studied due to its strong correlation with blood and heart diseases. Both dietary cholesterol and that are synthesized *de novo* are transported by the circulation in lipoproteins [13]. Familial hypercholesterolemia (FH) is a genetic hyperlipidemia that is characterized by high levels of plasma cholesterol carried by low-density lipoprotein (LDL) [14]. LDL is the main cholesterol transport protein in plasma, and the endocytosis of cholesterol-rich LDL can be mediated by LDL receptor (LDLr) [14]. FH is most commonly caused by mutations in the gene encoding the LDLr. It is also caused by mutations in three more genes encoding Apoprotein B-100, ARH adaptor protein, and PCSK9 protease [14].

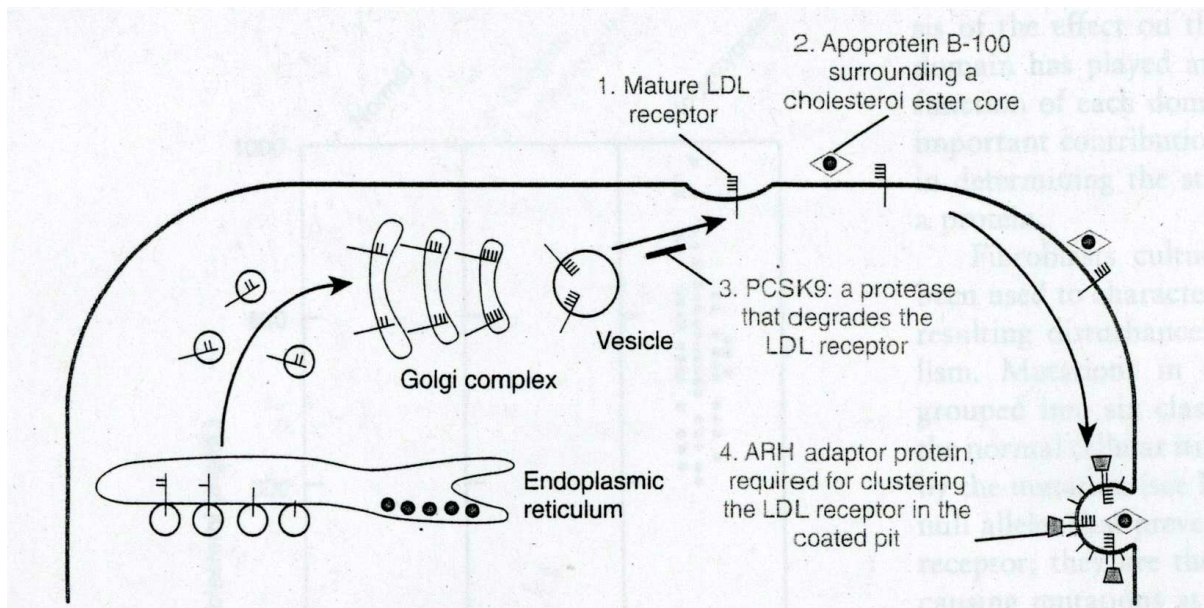


Figure 17. The four proteins associated with familial hypercholesterolemia. LDLr forms a complex with Apoprotein B-100 surrounding a cholesterol ester core. In the presence of ARH adaptor protein, the complex enters the cell by the endocytosis of the coated pit. Adapted from Nussbaum et al [14].

As shown in Figure 17, in the process of cholesterol uptake by the LDLr, a cholesterol ester core is surrounded by apoprotein B-100 to form a protein moiety of LDL. The mature LDLr binds the moiety, travels to the coated pits, and then enters the

cell by endocytosis of the coated pits in the presence of ARH adaptor protein. Once it enters the cell, LDL is hydrolyzed to release free cholesterol. Therefore, mutations in the genes encoding LDLr, Apoprotein B-100, PCSK9 and ARH adaptor protein can affect the cholesterol uptake by the LDLr [11]. The removal of LDL cholesterol from circulation can be reduced by mutation of LDLr, impairing LDL-LDLr binding caused by mutations in apoprotein B-100, or impairing the internalization of the LDL-LDLr complex caused by mutations in the ARH protein, or degradation of the LDLr caused by the mutations in PCSK9 [14].

According to Nussbaum et al, “the LDLr is a transmembrane glycoprotein mainly expressed in the liver and adrenal cortex, and plays a key role in cholesterol homeostasis. Hepatic LDLr clears about 50% of intermediate-density lipoproteins (IDL) and 66% to 80% of LDL from the circulation by endocytosis [14]”. It is worth the effort of studying the LDLr since elevated plasma LDL levels cause atherosclerosis.

2% ~ 10% LDLr mutations are large insertions, deletion, or rearrangement mediated by recombination between Alu repeats within LDLr [14]. These mutations decrease the efficiency of IDL and LDL endocytosis, resulting in increasing production of LDL from IDL, and decreasing hepatic clearance of LDL. Therefore, the clearance of LDL through LDLr-independent pathways is increased, resulting in atherosclerosis [14]. The effect of LDL receptor mutations on LDL plasma levels depends on environment, gender, and genetic background. Diet is the major environment modifier of LDL plasma levels because dietary cholesterol suppresses the synthesis of LDL receptors and thereby raises plasma LDL levels [14].

It has been reported that a mutation in PCSK9 is involved in autosomal dominant hypercholesterolemia (ADH), a rare form of FH without mutations of LDLr and the ligand binding domain of apoprotein B-100 [15].

PCSK9 has cytogenetic location: 1p32.3 and molecular location on chromosome 1: base pairs 55,505,148 to 55,530,525 [16]. An enzyme encoded by the PCSK9 gene in humans has orthologs found across many species. Increased PCSK9 protease activity causes the degradation of LDL receptor, thereby lowers the level of the receptor in hepatocytes, and regulates the LDL cholesterol metabolism [15]. Gain-of-function

missense mutations in the gene encoding PCSK9 enhance the activity of the PCSK9 protein, and cause FH. Loss-of-function mutations in the PCSK9 gene lead to an increase in the number of LDLr on the surface of liver cells. Hence, the amount of cholesterol circulating in the bloodstream is lowered [15]. As shown in Figure 18, in the cell PCSK9 interacts with LDLr for degradation through two pathways. In the first pathway, PCSK9 is secreted from cells, and then the extracellular PCSK9 internalized with the LDLr [15]. Bottomeley and coworkers studied the interaction of PCSK9 with LDLr, and found that PCSK9 binds LDLr at the first epidermal growth factor-like repeat homology domain (EGF-A) of LDLr [17]. Mutations in EGF-A inhibit the degradation of LDLr. It is also been found that PCSK9 dimers were more effective than PCSK9 monomer in degrading LDLr, and acidic endosomal pH increases the binding of PCSK9 with LDLr [15].

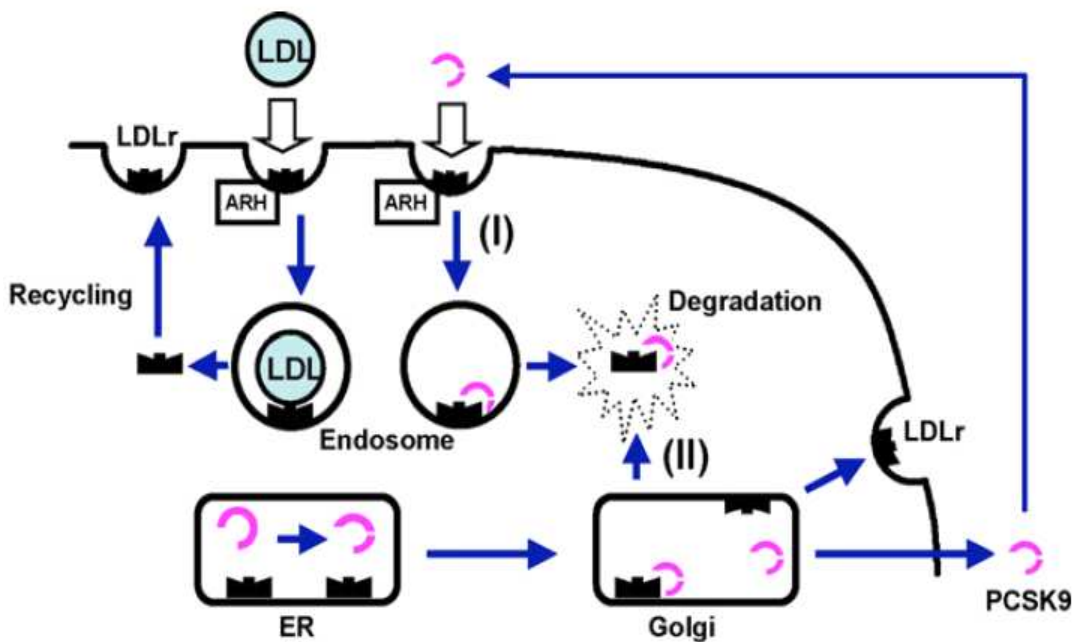


Figure 18. Two Pathway of PCSK9. Adapted from G. Lambert et al [15].

In the second pathway, PCSK9 acts on the LDLr after its biosynthesis before it reaches the basolateral surface of the cell [15].

PCSK9 is one of many secreted proteins that are essential for the regulation of biological activity are initially synthesized as inactive precursor proteins and are

subsequently proteolytically converted in the secretory pathway to the mature active forms [18]. These proteinases are called subtilisin-like proprotein convertases (SPCs) or protein convertases (PCs) because they have subtilisin-like catalytic domain [18]. Protein convertases are divided into S8A and S8B subfamilies. S8B contains seven closely related core members including subtilisin/kexin PCSK1, PCSK2, furin, PCSK4, PCSK5, PCSK6, PCSK7, while S8A contains more distantly related endoproteinases SKI-1/S1P, PCSK9 [19]. The pro-PCs contain multi domains including a signal peptide, a catalytic domain, a pro-domain, P-domain, a cysteine-rich domain, transmembrane domain and cytosolic domain. Each domain has its unique function. The signal peptide directs translocation into endoplasmic reticulum (ER); the pro-domain has intramolecular chaperone functions that direct compartment-specific activation, assist in folding of molecules, disassociate after the second internal cleavage event, and may autoinhibit PCs in select circumstances; the catalytic domain that contains the conserved catalytic triad that consists of aspartate, histidine and serine; the P-domain may stabilize acidic prodomain and catalytic domain, and is required for catalytic activity; a cysteine-rich domain confers protein-protein interaction properties, and directs cell-surface tethering; the transmembrane domain and cytosolic domain direct PC sorting and transit control within cell compartments. Transmembrane and cytosolic domains are present only in furin, PCSK5, PCSK6, PCSK7 [19].

Proprotein convertases activate a broad range of distinct proteins. PCSK1 and PCSK2 activate polypeptide prohormones; Furin activates multiple mammalian and microbial precursor proteins; PCSK4 activates proteins involved in sperm motility, reproduction; PCSK5 and PCSK6 activate ECM proteins; PCSK7 activates multiple precursors; SKI-1/S1P processes membrane-bound transcription factors involved in lipid metabolism; and PCSK9 regulates plasma LDL levels through increased degradation of LDLr proteins [19]. Physiologically important proteins may require activation by means of post-translational cleavage of an inactive precursor molecule. The deficiency of PCSK1 or PCSK2 results in abnormal glucose homeostasis, and impaired prohormones processing. PCSK1, PCSK2, furin, PCSK5, PCSK6, PCSK7 have been associated with cancers through the complex interactions among their activated substrate [19]. PCs also relate to

infectious diseases and lipid disorders, atherosclerosis and Alzheimer's disease, and biodefense. Therefore, PCs are potential therapeutic targets [19].

According to Lambert et al., "PCSK9 is synthesized as a 72-kDa protein of 692 amino acids in which the signal peptide (residues 1-30) and the prodomain (residue 31 – 152) of PCSK9 precedes a catalytic domain (residues 153 – 451), that contains the canonical D186, H226 and S386 catalytic triad as well as the oxyanion hole N317 residue, followed by a C-terminal domain (residues 452 – 692) [15]".

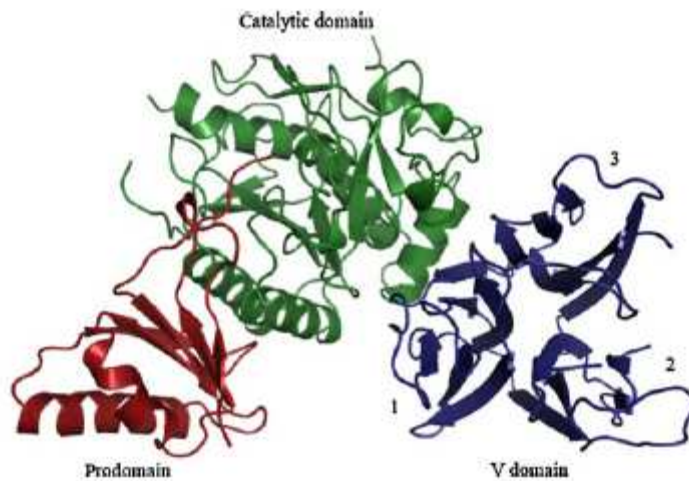


Figure 19. Ribbon structure of PCSK9. Adapted from G. Lambert et al [15].

As shown in Figure 19, the prodomain consists of two α helices and a four-stranded antiparallel β sheet. The prodomain associates with catalytic domain through hydrophobic and electrostatic interactions [15]. PCSK9 autocatalytically cleaves the peptide bond after non-basic amino acids between Gln152 and Ser153 to generate a 14-kDa prodomain and a 63-kDa moiety [15]. The prodomain are permanently associated with the 63 kDa PCSK9 moiety, and the four C-terminal amino acids of the prodomain (residues 149 – 152) bind in the catalytic site and further inhibit the catalytic activity by N-terminus extension of the prodomain [19]. The catalytic domain consists of seven-stranded parallel β sheet and α helices. The catalytic triad of PCSK9 consists of residues Asp186, His226, and Ser386. PCSK9 does not act as a catalyst but as a chaperone that binds the LDLr at its epidermal growth factor-like repeat A (EGF-A) for lysosomal

degradation [15]. The V domain of PCSK9 consists of three barrel-like subdomains that are made up of antiparallel β strands, and stabilized by three internal disulfide bonds [15]. The V domain is rich in histidine residues that can control the pH-dependent protein-protein interactions [15].

Researchers have been studying how the mutations in PCSK9 relate to FH. They reported the disease-associated variants in a database at www.ucl.ac.uk/ [20]. As shown in Figure 20, the mutations of PCSK9 can be found in any domains of PCSK9.

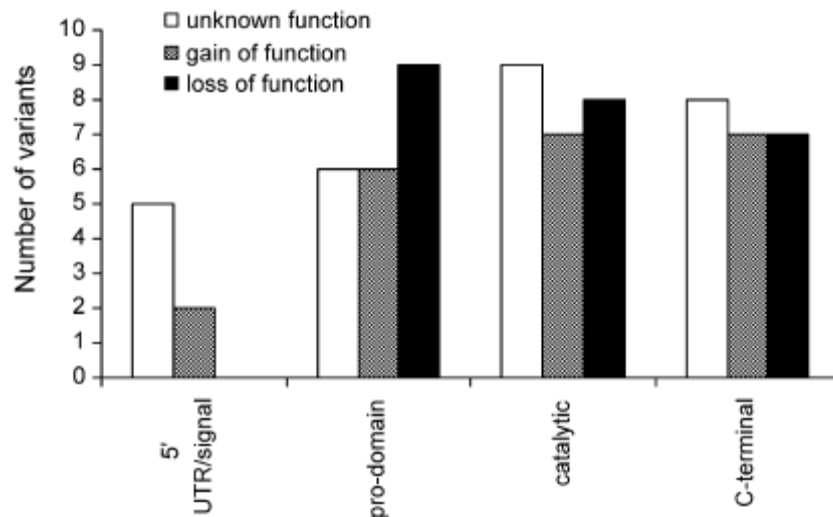


Figure 20. Number of variants in each domain of the PCSK9 gene according to putative function (n = 73). Intronic variants have not been included. Adapted from Leigh et al [20].

The selected naturally occurring variants are summarized in Table 2. The loss-of-function mutations include L82X, Y142X, C679X, DR97, G106R, L253F, N157K and H391N, while the gain-of-function mutations include D374Y, D374H, S127R, D129G, F216L, and R218S [15].

The function of PCSK9 is physiologically significant, and it is clinically relevant to measure circulating levels of PCSK9 and to study pharmacological factors affecting its secretion. It has been reported that plasma PCSK9 levels correlate positively with LDL cholesterol but not with HDL cholesterol or TG in healthy donors [15]. PCSK9 has become a validated target for the treatment of hypercholesterolemia and associated cardiovascular diseases. Study suggests that pharmacologic interventions that inhibit

PCSK9 may be safe. The first approach to inhibit PCSK9 include targeting PCSK9 mRNA that involves the delivery of single-stranded antisense DNA-like chimeric oligonucleotides via an RNaseH-mediated pathway, and injection of liposomal double stranded RNA-like siRNAs that interact with the RNA-interference silencing complex [19, 20, 21].

Table 2. PCSK9 naturally occurring variants (X represents stop codon) [20, 22].

| Protein | Domain | Effect | Wild | | Mutant | |
|-------------|-------------------|---|---------------|----------------|---------------|----------------|
| | | | AA type | hydrophobicity | AA type | hydrophobicity |
| p.Arg46Leu | Pro-domain | Loss of function, decreased phosphorylation of Ser47 | basic | -14 | aliphatic | 97 |
| p.Leu82X | Pro-domain | Loss of function, truncated peptide, disrupt proper folding | aliphatic | 97 | X | |
| p.Arg97del | Pro-domain | Loss of function, disrupts the fold of the entire prodomain. | basic | -14 | | |
| p.Gly106Arg | Pro-domain | Loss of function, improper orientation of the beta-strands. | unique | 0 | basic | -14 |
| p.Ser127Arg | Pro-domain | Gain of function, | polar neutral | -5 | basic | -14 |
| p.Asp129Gly | Pro-domain | Gain of function | acidic | -55 | unique | 0 |
| p.Tyr142X | Pro-domain | Loss of function, truncated peptide, disrupt proper folding | aromatic | 63 | X | |
| p.Asn157Lys | Catalytic | Loss of function, could break hydrogen bond and then destabilize the packing of this helix | polar neutral | -28 | basic | -23 |
| p.Phe216Leu | Catalytic | Gain of function can't undergo the second cleavage that can't not induce LDLr degradation. | aromatic | 100 | aliphatic | 97 |
| p.Arg218Ser | Catalytic | Gain of function can't undergo the second cleavage that can't not induce LDLr degradation. | basic | -14 | polar neutral | -5 |
| p.Leu253Phe | Catalytic | Loss of function, results in a PCSK9 protein that is defective in autoprocessing. | aliphatic | 97 | aromatic | 100 |
| p.Asp374Tyr | Catalytic | Gain of function, increases in affinity for LDLr by Hydrogen bonding or pi stacking with H306 of EGF-A. | acidic | -55 | aromatic | 63 |
| p.Asp374His | Catalytic | Gain of function, increases in affinity for LDLr by Hydrogen bonding or pi stacking with H306 of EGF-A. | acidic | -55 | basic | 8 |
| p.Cys679X | C-terminal domain | Loss of function, truncated peptide, disrupt proper folding | polar neutral | 49 | X | |

The second approach to inhibit PCSK9 directly by molecules includes antibodies or small interfering RNAs that interfere with PCSK9/LDLr interaction at the plasma membrane, inhibitors of PCSK9 catalytic activity within the ER, other proprotein convertases that enhance PCSK9 cleavage, and molecules that destabilize the PCSK9 structure to mimic loss of function mutants [19, 23]. A list of inhibitors of PCSK9

currently undergoing development to reduce the LDL-C levels are summarized in Table 3 [24]. It has been reported that an antibody for PCSK9 (mAb1) administered to wild-type mice doubled the hepatic content of LDLR and reduced serum total cholesterol by 36% [24]. Cynomolgus monkeys treated with a single dose of PCSK9 siRNA had a mean reduction in LDL-C levels of 56% [24].

Table 3: PCSK inhibitors under development [24].

| Company | Name of agent | Stage of development | Comments |
|---|---------------|----------------------|---|
| Monoclonal antibodies | | | |
| Merck ⁸⁹ | 1D05-IgG | In development | Rhesus monkeys; results presented at the 2009 AHA scientific sessions |
| Sanofi-Aventis–Regeneron ¹⁰¹ | REGN727 IgG | Phase I | Phase I results published online May 2010; LDL decreased 60% |
| Pfizer–Rinat ¹⁰² | RN316 IgG | Phase I | Clinical trial started |
| Amgen ¹⁰³ | mAb1-IgG | In development | Cynomolgus monkeys |
| Antisense oligonucleotides | | | |
| Santaris ⁹³ | SPC5001 | In development | LNA class ASO |
| Alnylam ⁹⁶ | ALN-PCS | In development | Liposomal formula, Cynomolgus monkeys, PNAS August 2008 ⁹¹ |
| BMS–ISIS ^{104,105} | BMS-844421 | Phase I | |
| Adnectin | | | |
| BMS–Adnexus ¹⁰⁶ | BMS-962476 | Preclinical | |
| Abbreviations: ASO, antisense oligonucleotide; LNA, locked nucleic acid; PNAS, <i>Proceedings of the National Academy of Sciences</i> . | | | |

Many other PCs have been studied, especially furin. Comparative study of PCSK9 with well characterized furin and other PCs will be an efficient way to get information about PCSK9.

II. Comparative study of PCSK9 with other PCs

Sun and coworkers reported that the multiple sequence alignment of PCSK9 with furin and three PCs (PCSK4, PCSK5 and PCSK6) using Clustal2 shows that PCSK9 is closely resemble to furin [25]. When they compared the key residues in the binding pocket of furin and those in PCSK9, they found that the obtained multiple sequence alignment indicated the mutations of PCSK9 including N192 → S, R193 → -, E230 → Q, V231 → G, E257 → -, A267 → L, S319 → G, S343S → L, P372 → A.

The 3D structure of the furin catalytic domain with an inhibitor complex (Protein Data Bank ID: IP8J) was created with Chimera 1.6 (Figure 21) [26].

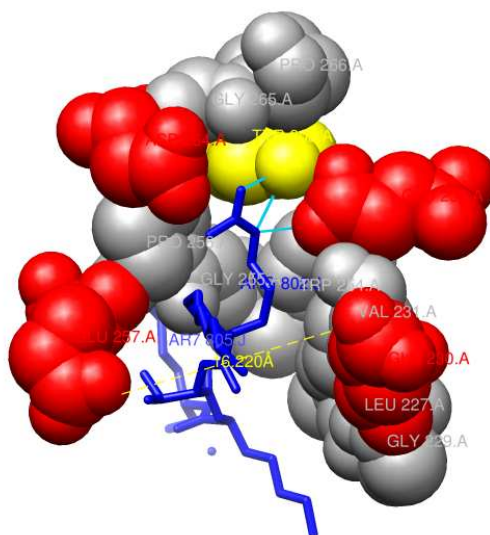


Figure 21. Furin Binding Pocket. Adapted from Sun, et al [25].

The sensitivity and the compensatory effect of the positive charge at substrate positions P4-P6 requires negatively charged residues in the binding pocket of PCs [25]. Negatively charged residues at position 230 and 257 play a key role in regulation of the substrate specificity of mammalian proprotein convertases since they interact with a positively charged residue at substrate position P5 or P6, and facilitate flexible interactions in this region [25]. It has been reported that cleavage of proprotein convertases can be inhibited by a small molecule characterized by positively charged

residues at substrate position P1, P2, and P4 [25]. This small molecule dec-RVKR-cmk efficiently binds to all seven 8B proprotein convertases [25]. This methodology can be used to study the substrate specificity of PCSK9 and find its small molecule inhibitor.

MEGA is used to build a phylogenetic tree for PCSK9 from different species [27].

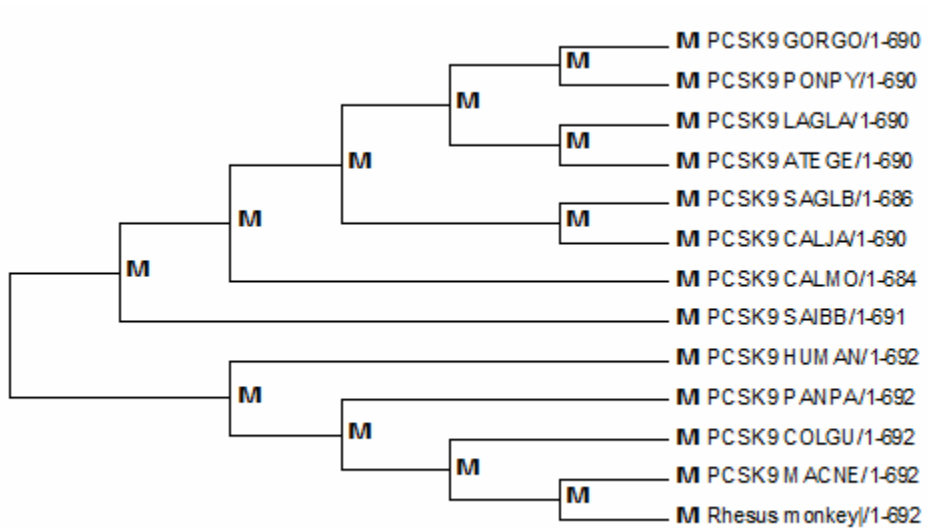


Figure 22 shows the resulting phylogenetic tree.

The information on PCSK9 is valuable, and can be obtained from the PDB website <http://www.rcsb.org/pdb/home/home.do>. Table 4 summarizes a list of solved structures of PCSK9 [28].

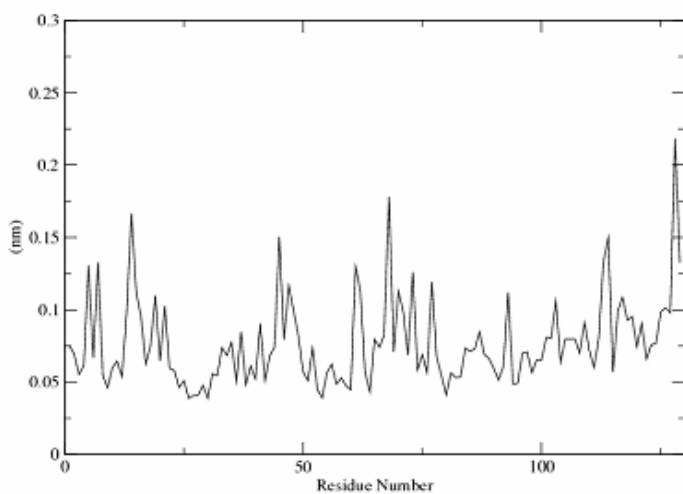
Table 4: Solved PCSK9 Structure in PDB

| PDB ID | Structure Title |
|----------------------|---|
| 2NP9 | Crystal structure of a dioxygenase in the Crotonase superfamily |
| 2P4E | Crystal Structure of PCSK9 |
| 2PMW | The Crystal Structure of Proprotein convertase subtilisin kexin type 9 (PCSK9) |
| 2QTW | The Crystal Structure of PCSK9 at 1.9 Angstroms Resolution Reveals structural homology to Resistin within the C-terminal domain |
| 2W2M | WT PCSK9-DELTAC BOUND TO WT EGF-A OF LDLR |
| 2W2N | WT PCSK9-DELTAC BOUND TO EGF-A H306Y MUTANT OF LDLR |
| 2W2O | PCSK9-DELTAC D374Y MUTANT BOUND TO WT EGF-A OF LDLR |
| 2W2P | PCSK9-DELTAC D374A MUTANT BOUND TO WT EGF-A OF LDLR |
| 2W2Q | PCSK9-DELTAC D374H MUTANT BOUND TO WT EGF-A OF LDLR |
| 2XTJ | THE CRYSTAL STRUCTURE OF PCSK9 IN COMPLEX WITH 1D05 FAB |
| 3BPS | PCSK9:EGF-A complex |
| 3GCW | PCSK9:EGFA(H306Y) |
| 3GCX | PCSK9:EGFA (pH 7.4) |
| 3H42 | Crystal structure of PCSK9 in complex with Fab from LDLR competitive antibody |
| 3M0C | The X-ray Crystal Structure of PCSK9 in Complex with the LDL receptor |
| 3P5B | The structure of the LDLR/PCSK9 complex reveals the receptor in an extended conformation |
| 3P5C | The structure of the LDLR/PCSK9 complex reveals the receptor in an extended conformation |

Although the number of solved structures is limited, it may take researchers weeks or months to build the model from the x-ray experimental data. When the molecule becomes larger and larger, the disadvantage of the experimental method becomes obvious. The molecular dynamics simulation could be a reasonable method for the study of PCSK9.

III. Molecular Dynamic Simulation Results

We have performed MD on lysozyme (1AKI), and analyzed the trajectory with GROMACS tool `g_rmsf` to get its fluctuation information, and with our program to get the rigidity profile (Figure 23).



Force Constant Profile for Lysozyme (pdbId: 1AKI)

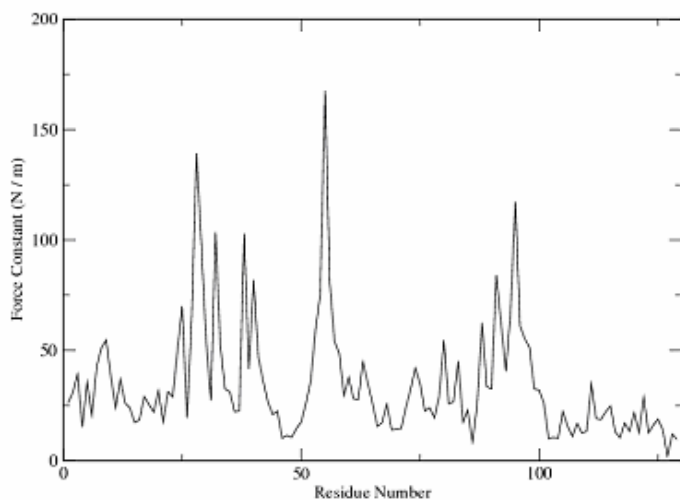


Figure 23. Fluctuation and rigidity profile of the Lysozyme (1AKI). The simulation is 5 ns MD run with GROMACS.

Figure 23 represents the fluctuation and rigidity profile of lysozyme. As seen on the figure, the residues with high fluctuation often have low rigidity. For example, the strong rigidity peak is located in the #50 – #55 region where fluctuation is small. This result confirms our program can correctly predict the rigidity of the residues. We plotted the rigidity data with our program (Figure 24). We also labeled the predicted high rigidity residues including Trp28, Ala32, Phe38, Thr40, Ile55, Ser91, and Ala95 in Chimera image of lysozyme (Figure 25) [29].

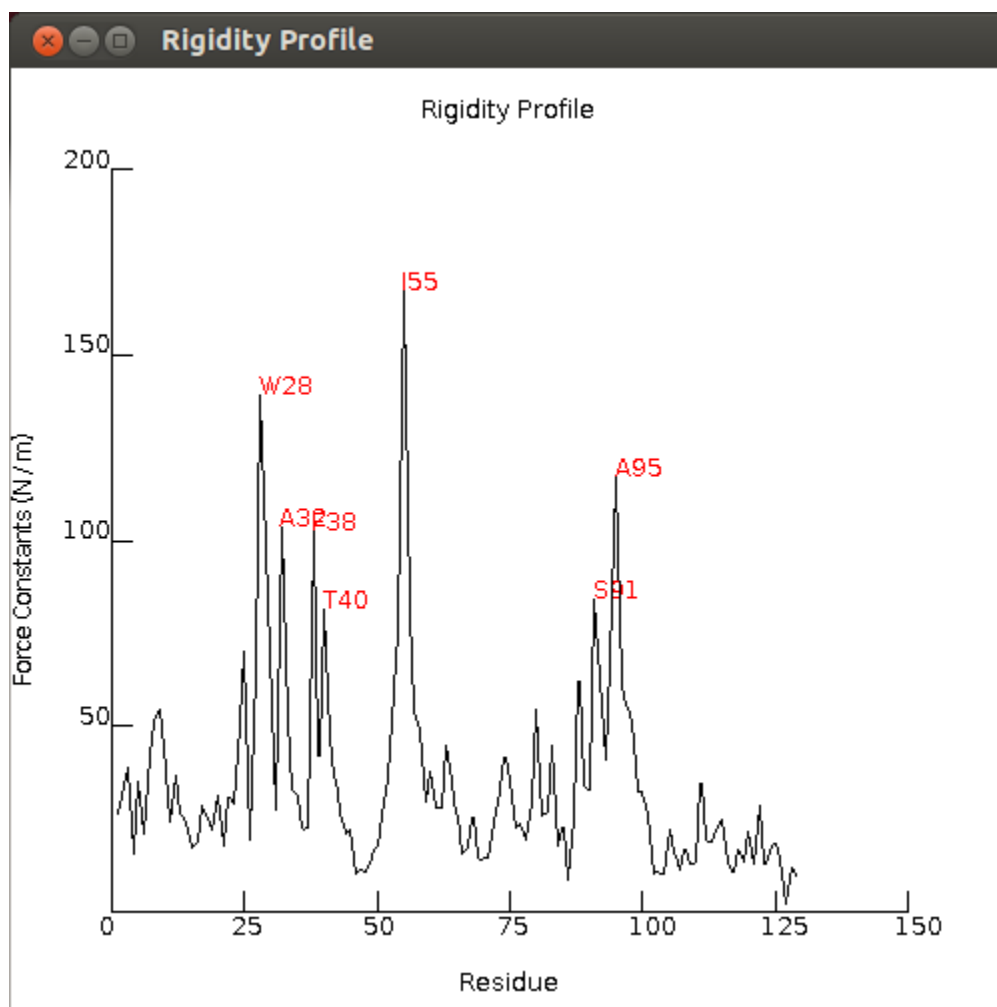


Figure 24. Rigidity profile plotted with our program.

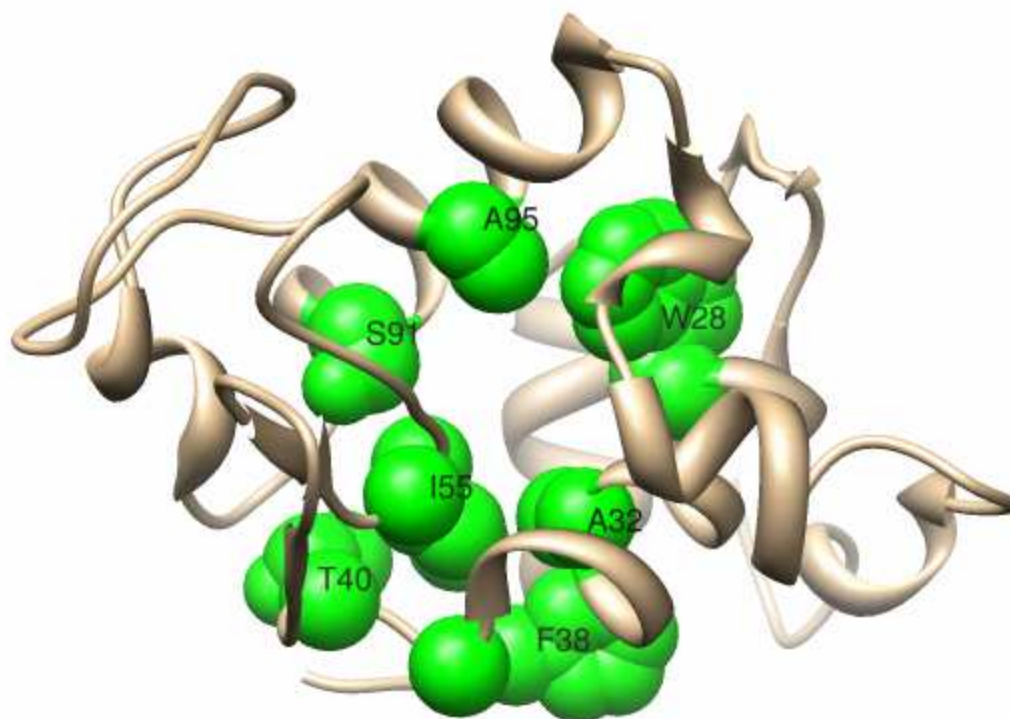


Figure 25. Residues with high rigidity predicted by our program are Trp28, Ala32, Phe38, Thr40, Ile55, Ser91, and Ala95. These residues are labeled with 1 letter code and shown in sphere shapes in the Chimera image of lysozyme (1AKI).

Our program allows the users to easily locate the amino acid residues with high rigidity by labeling those amino acids above the threshold value set by the user (the default value is 50% of the maximum value). Both fluctuation and rigidity information would help us to understand the property of the biological molecule. It has been found that three amino acid positions beneath the active site are occupied by Thr 40, Ile 55, and Ser 91 in hen, pheasant, and other avian lysozymes [30] with experimental methods. These three amino acids can be found among the amino acids with high rigidity predicted by our program.

The above result on lysozyme indicates our program could be used in the study of other proteins such PCSK9. We performed the similar study on PCSK9 (PDB code: 2P4E) (Figure 26). Since PCSK9 is a bigger protein with some missing residues in the initial configuration, we will focus on analyzing the region (#219 – #449) with the longest unbroken sequence (Figure 27). Within this region, L286, T313, V336, A363,

T385, A389 and V392 are predicted to have high rigidity, and there is no reporting mutation among them [20]. The result indicates the rigidity profile could predict the conserved region of the protein.

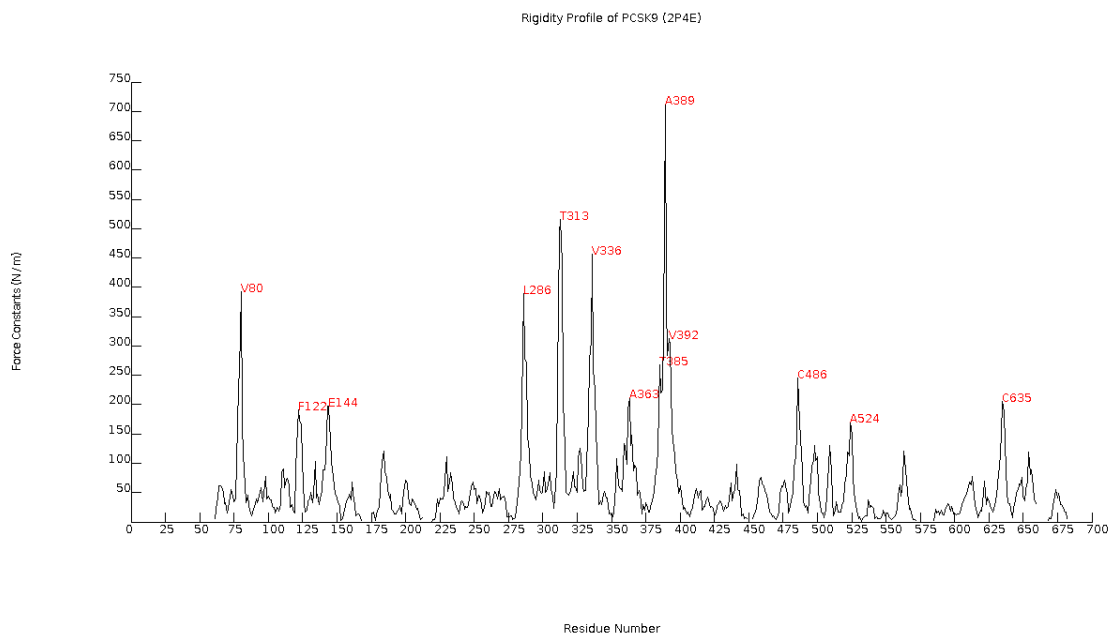


Figure 26. PCSK9 (1AKI) rigidity profile with missing residues located in the disconnected region in the graph. The simulation is 10 ns MD run with GROMACS.

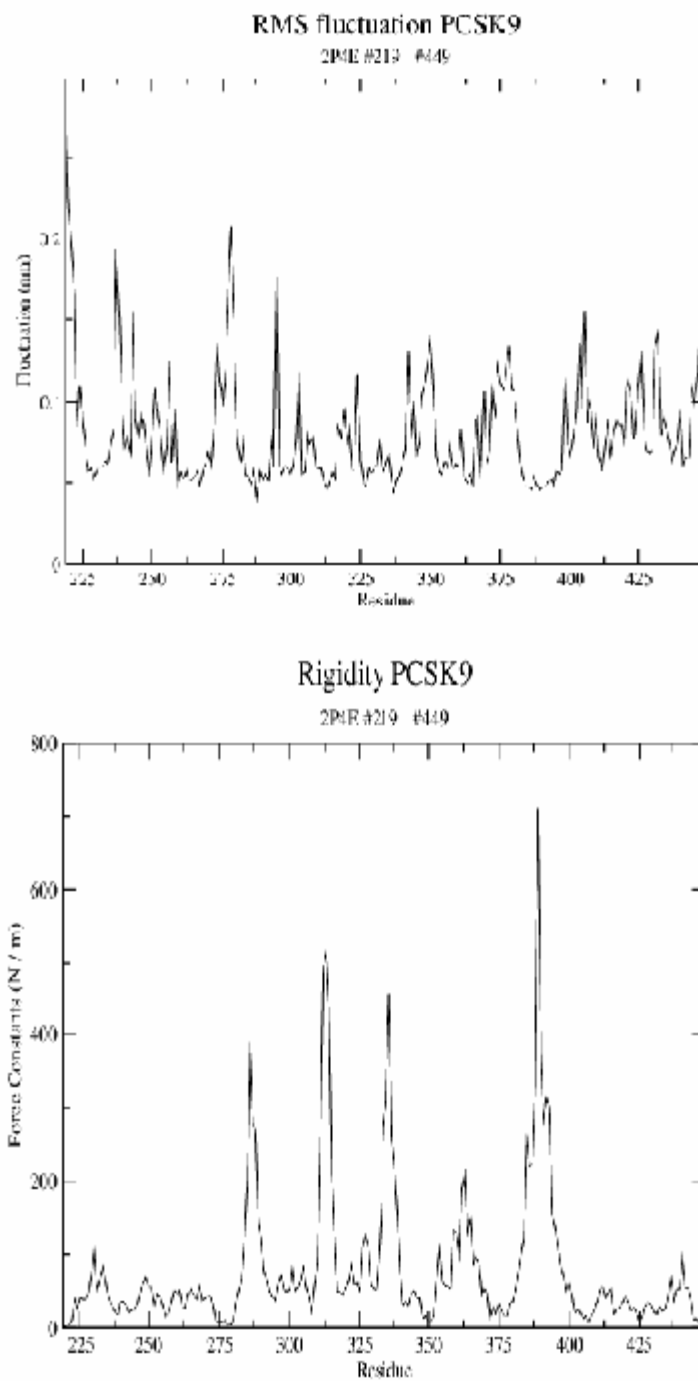


Figure 27. The fluctuation and rigidity profile of PCSK9 partial sequence (#219 - #449).

It has been reported that D374 is the binding location where the PCSK9 forms the complex with LDLr, and its mutations change its binding efficiency with LDLr [17].

Figure 27 indicates D374 has high fluctuation and low rigidity result. We also labeled the predicted high rigidity residues including L286, T313, V336, A363, T385, A389, and V392 in Chimera image of PCSK9 (Figure 28) [29].

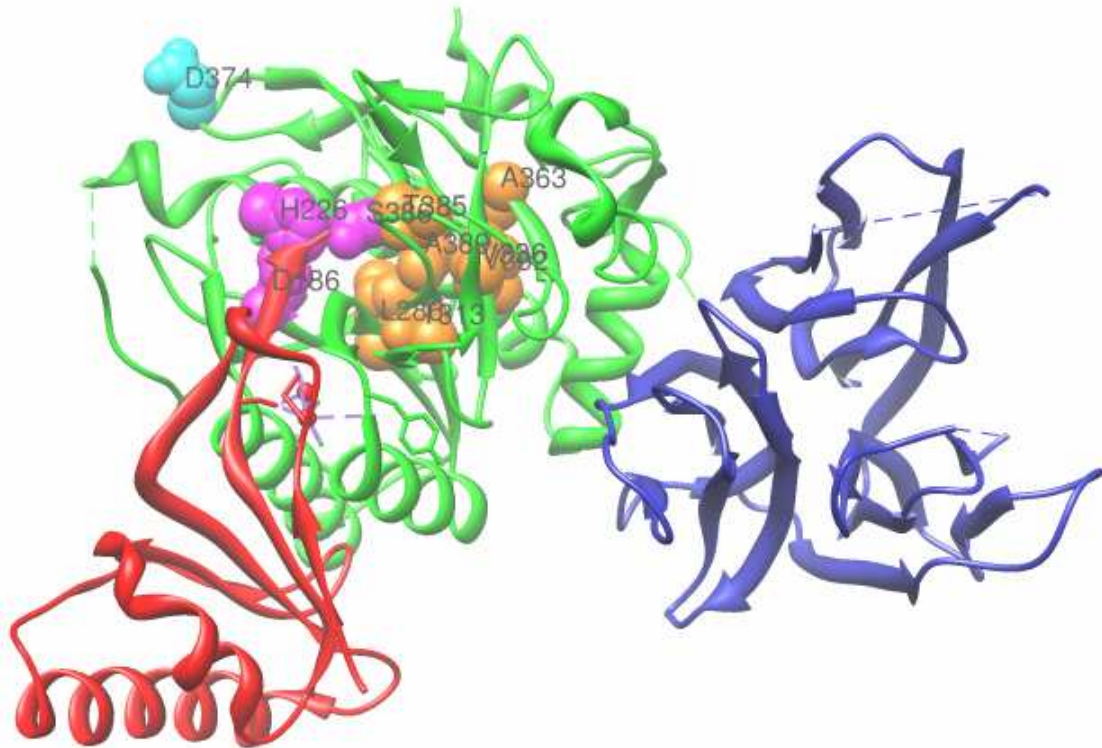


Figure 28. Residues with high rigidity predicted by our program are L286, T313, V336, A363, T385, A389, and V392. These residues are labeled with 1 letter code and shown in sphere shapes and located in the center of the A chain in the Chimera image of PCSK9 (2P4E). The triad residues located on the left of the center, and D374 are also labeled.

We need more analysis on the pattern of the fluctuation and rigidity on other residues to find the important information about the binding of the PCSK9 and the LDLr.

5. Conclusions

In this project, we learned how to use GROMACS in molecule dynamics simulations. Through the molecule dynamics simulation of lysozyme using GROMACS, we understood that the process of running GROMACS in protein dynamics simulations involves many steps, and GROMACS does not provide a tool to analyze the rigidity of the protein.

We have developed a Java application to simplify the steps involved in GROMACS. We investigated two methods that allow us to call C code from Java, and we decided to use Java Runtime class method since JNI method is too complicated to implement. Through the graphical user interface (GUI), users can easily carry out molecular dynamics simulations using GROMACS with their own settings or simply accepting the default settings given by the program. Our program also allows users to analyze the GROMACS trajectories to generate the rigidity of the protein, and then plot the rigidity profile graph with our built-in plotting feature. Compared to JGromacs, our program has better performance, and works well with the large trajectory files.

We tested our program with lysozyme, and obtained promising results that show the amino acids involved in the active site of the lysozyme are among the amino acids with high rigidity. We also used our program in the molecular dynamics simulation of PCSK9, and found that the amino acids with high rigidity are not among the amino acids that have reported mutations. These results indicate our program could be used to find the active site and the conserved amino acids in the protein.

6. Future Work

A possible extension of this work would be to continue validating the program with well studied lysozyme and its variants. This would enable us to find a method to determine the relationship between the simulation results and the protein property, which would allow us to expand our study to PCSK9 and its complexes with LDLr to determine its role in cholesterol metabolism.

Another extension would be to develop a web application of this program that would allow remote users to access the program.

7. References

- [1] www.ch.embnet.org/MD_tutorial/ (last retrieved on Feb 1, 2012).
- [2] McCammon J.A., Gelin B.R., and Karplus M. *Nature* 267, 585 (1977).
- [3] http://cinjweb.umdj.edu/~kerrigje/pdf_files/fwspidr_tutor.pdf (last retrieved on Sep 5, 2012).
- [4] Stadler AM, Garvey CJ, Bocahut A, Sacquin-Mora S, Digel I, Schneider GJ, Natali F, Artmann , Zaccai G, *J. R. Soc. Interface*, 2012 Jun 13.
- [5] Munz M., Biggin P.C., *J. Chem. Inf. Model.* 2012, 52, 255-259.
- [6] van der Spoel D., Lindahl E. Hess B., Groenhof G., Mark A.E., and Berendsen H.J.C., *J. Comput. Chem.* 26 (16): 1701-18.
- [7] Gromacs 4.5 Online Reference, manual.gromacs.org/current/ (last retrieved on Nov 1, 2012).
- [8] van der Spoel D., Lindahl E. Hess B., van Buuren A.R., Apol E., Meulenhoff P.J., Tieleman D.P., Sijbers A.L.T.M., Feenstra K.A., van Drunen R., and Berendsen H.J.C., *Gromacs User Manual version 4.5.4*, www.gromacs.org (last retrieved on Nov 1, 2012).
- [9] <http://www.bevanlab.biochem.vt.edu/Pages/Personal/justin/gmx-tutorials/lysozyme/index.html> (last retrieved on Nov 1, 2012)
- [10] <http://www.ibm.com/developerworks/java/tutorials/j-jni/section2.html> (retrieved on Dec 3, 2012).
- [11] Gamma E., Helm R., Johnson R., Vlissides J. *Design Patterns: Elements of Reusable Object-Oriented Software*, 1995, Addison-Wesley.

- [12] <http://csis.pace.edu/~bergin/mvc/mvcgui.html>. (last retrieved on Nov 1, 2012)
- [13] Nelson DL, Cox MM. 2004. *Lehninger Principles of Biochemistry*, 4th edition. Chapter 21.
- [14] Nussbaum, McInnes, Willard. 2007. *Genetics in Medicine*.
- [15] Lambert G, Charlton F, Rye K, Piper D, Molecular basis of PCSK9 function, *Atherosclerosis*, 2009; 203:1-7.
- [16] <http://ghr.nlm.nih.gov/gene/PCSK9>. (last retrieved on Feb 1, 2012)
- [17] Bottomley M, et al. Structural and Biochemical Characterization of the Wild Type PCSK9-EGF(AB) Complex and Natural Familial Hypercholesterolemia Mutants, *J. Biol. Chem.*, 284 (2009) 1313-1323.
- [18] Henrich S, Lindberg I., Bode W., Than M.E., *J. Mol. Biol* (2005) 345, 211-227.
- [19] Artenstein A, Opal SM, Proprotein Convertases in Health and Disease, *The New England Journal of Medicine*, 2011; 365; 26:2507-2518.
- [20] Leigh et al. Commentary PCSK9 variants: A new database, *Atherosclerosis*, 203 (2009) 32-33.
- [21] Benjannet et al. The Proprotein Convertase (PC) PCSK9 Is Inactivated by Furin and/or PC5/6A, *Journal of Biological Chemistry*, Oct. 2006, vol281(41), page 30561 – 30571.
- [22] <http://www.sigmaaldrich.com/life-science/metabolomics/learning-center/amino-acid-reference-chart.html> (retrieved on Sep 1, 2012).
- [23] Lou KJ, 2009, The secreted secret of PCSK9, *SciBX* 2(22).
- [24] Brautbar, Ballantyne, Pharmacological strategies for lowering LDL cholesterol:

statins and beyond. *Nature Reviews Cardiology*, vol 8, May 2011, page 253 – 265.

- [25] Sun et al, Comparative study of the binding pockets of mammalian proprotein convertases and its implications for the design of specific small molecule inhibitors, *Int. J. Biol. Sci.* 2010; 6:89-95.
- [26] Pettersen EF, Goddard TD, Huang CC, Couch GS, Greenblatt DM, Meng EC, Ferrin TE. *J Comput Chem.* 2004 Oct;25(13):1605-12.
- [27] Tamura K., Peterson D., Peterson N., Stercher G., Nei M., Kumar S., *Molecular Biology and Evolution* 28: 2731-2739.
- [28] www.rcsb.org/pdb/home/home.do (last retrieved on Sep 1, 2012).
- [29] [UCSF Chimera--a visualization system for exploratory research and analysis.](#)
Pettersen EF, Goddard TD, Huang CC, Couch GS, Greenblatt DM, Meng EC, Ferrin TE. *J Comput Chem.* 2004 Oct;25(13):1605-12.
- [30] Lescar J., Souchon H., Alzari P.M., *Protein Sci.* 1994 May; 3(5): 788–798.